Fermi National Accelerator Laboratory
FERMILAB-Pub-95/021-A
March, 1995

Oscillons: Resonant Configurations During Bubble Collapse

E. J. Copeland[1], M. Gleiser*[2], and H.-R. Müller[3]

[1] *School of Mathematical and Physical Sciences, University of Sussex*

Brighton BN1 9QH, UK

[2] *Nasa/Fermilab Astrophysics Center*

Fermi National Accelerator Laboratory

P.O.Box 500, Batavia, IL 60510, USA

[3] *Department of Physics and Astronomy, Dartmouth College*

Hanover, NH 03755, USA

(SUSX-TH-95/3-3 Fermilab-Pub-95/021-A DART-HEP-95/01 hep-ph/9503217)

Abstract

Oscillons are localized, non-singular, time-dependent, spherically-symmetric solutions of nonlinear scalar field theories which, although unstable, are *extremely* long-lived. We show that they naturally appear during the collapse of subcritical bubbles in models with symmetric and asymmetric double-well potentials. By a combination of analytical and numerical work we explain several of their properties, including the conditions for their existence, their longevity, and their final demise. We discuss several contexts in which we expect oscillons to be relevant. In particular, their nucleation during cosmological phase transitions may have wide-ranging consequences.

PACS: 98.80.Cq, 64.60.Cn, 64.60.-i, 11.10.Lm

---

*NSF Presidential Faculty Fellow. On leave from Department of Physics and Astronomy, Dartmouth College, Hanover NH 03755.

I. INTRODUCTION

The search for static, localized, non-singular solutions of nonlinear field theories has by now a long history [1]. In (1+1)-dimensions, it is possible to find exact static solutions to the nonlinear Klein-Gordon field equations for certain interacting potentials, such as the kink solutions of sine-Gordon or ϕ^4 models. For a larger number of spatial dimensions, Derrick's theorem forbids the existence of static solutions for models involving only real scalar fields [2]. There are several ways to circumvent Derrick's theorem, by invoking more complicated models with two or more interacting fields. Well-known examples include topological defects such as the 't Hooft-Polyakov monopole or the Nielsen-Olesen vortices [3]. Topological conservation laws guarantee the stability of these configurations.

It is also possible to find localized time-dependent but non-dissipative solutions of nontopological nature, the so-called nontopological solitons [4]. The simplest model of a nontopological soliton in the context of renormalizable theories has a complex scalar field quadratically coupled to a real scalar field with quartic potential. The stability of the configuration comes from the conserved global charge Q carried by the complex field which is confined within a spherically-symmetric domain formed by the real scalar field. One can show that for Q larger than a critical value, the energy of the configuration is smaller than the energy of Q free particles. There has been a recent upsurge of interest on nontopological solitons due to their potential relevance to cosmology and astrophysics [5]. If one waives the requirement of renormalizability, it is possible to find nontopological solitons for models with a single complex scalar field, by invoking, e.g., a ϕ^6 term in the potential. These are the so-called Q-ball solutions discovered by Coleman and collaborators [6].

In the present work we will go back to the simple models involving only a self-interacting real scalar field and study the properties of *time-dependent* spherically-

symmetric solutions. Due to the constraint imposed by Derrick's theorem, these configurations have been somewhat overlooked in the literature (but not completely, as we will discuss below). Why should anyone bother with solutions which are known to be unstable? One possible answer is that instability is a relative concept, which only makes sense in context, that is, when the lifetime of a given configuration is compared with typical time-scales of the system under study. Thus, unstable but long-lived configurations may be relevant for systems with short dynamical time-scales. Another answer is that a detailed study of these configurations can greatly clarify dynamical aspects of nonlinearities in field theories and the rôle they play in several phenomena, ranging from nonlinear optics to phase transitions both in the laboratory and in cosmology [7].

One of the motivations for studying the evolution of unstable spherically-symmetric configurations comes from the work of Gleiser, Kolb, and Watkins on the rôle subcritical bubbles may play in the dynamics of weak first order phase transitions [8]. Considering models with double-well potentials in which the system starts localized in one minimum, these authors proposed that for sufficiently weak transitions correlation-volume bubbles of the other phase could be thermally nucleated, promoting an effective phase mixing between the two available phases even before the critical temperature is reached from above. This could have important consequences for models of electroweak baryogenesis which rely on the usual homogeneous nucleation mechanism [9]. However, Gleiser, Kolb, and Watkins did not include the shrinking of the bubbles in their estimate of the fraction of the volume occupied by each of the two phases, leading some authors to question their results [10]. Since then, Gleiser and Gelmini included the shrinking of the bubbles into the original estimates, concluding that for sufficiently weak transitions subcritical bubbles are indeed nucleated at a fast enough rate to cause substantial phase mixing [11]. Although an improvement, the modeling used to describe the bubble shrinking was still too simplistic, as it assumed that the bubbles just shrunk with constant velocity.

The evolution of spherically-symmetric unstable solutions of the nonlinear Klein-Gordon equation was originally studied numerically in the mid-seventies by Bogolubsky and Makhankov [12]. Using a quasiplanar initial configuration for the bubbles (that is, a $\tanh(r - R_0)$ profile, with R_0 the initial radius), these authors discovered that for a certain range of initial radii the bubble evolution could be described in three stages; after radiating most of its initial energy the bubble settled into a regime which was quite long-lived, with a lifetime which depended on the initial radius. The bubble then disappeared by quickly radiating away its remaining energy. These configurations were called "Pulsons" by these authors, due to the pulsating mechanism by which they claimed the initial energy was being radiated away. Their results were recently rediscovered and refined by one of us [13]. After a more detailed analysis of these configurations, it became clear that their most striking feature was not the pulsating mechanism by which bubbles radiate their initial energy, but the rapid oscillations of the field's amplitude at the core of the configuration during the pseudo-stable regime, in a manner somewhat analogous to resonant breathers in kink-antikink scattering [14]. In fact, it was realized that during the pseudo-stable regime almost no energy is radiated away and the radial pulsation is actually quite small in amplitude. Hence the name "Oscillon" was proposed instead. It was also shown that these configurations appear both in symmetric and asymmetric potentials, are stable against small radial perturbations, and have lifetimes far exceeding naive expectations. However, not much else has been done in order to explore the properties of these configurations. Other works on this topic were concerned in establishing the existence of these solutions for other potentials, such as the sine-Gordon and logarithmic potentials, different symmetries, and somewhat limited stability studies [15].

By a combination of analytical and numerical methods, we will shed some light on the properties of these configurations (henceforth oscillons). We will establish the conditions —

for their existence, the reason for their longevity, and clarify their final collapse. Armed with a better understanding of their properties, we will also be able to suggest several situations where we believe oscillons can be of importance.

The rest of this paper is organized as follows. In the next Section we will set up the general formalism and obtain the exact solution of the spherically-symmetric linear Klein-Gordon equation. As expected, in the linear case no oscillons appear, with bubbles quickly decaying away. We obtain the time-scale in which this decay occurs in order to later compare it to the case when nonlinearities are present. In Section 3 we present the numerical results that establish several of the key properties of oscillons for symmetric double-well potentials. Guided by these results, in Section 4 we present analytical arguments to explain why there is a minimum initial radius for bubbles to settle into the oscillon stage, why some oscillons live longer than others, and how oscillons finally disappear. In Section 5 we extend the numerical analysis of Section 3 to asymmetric double-well potentials, showing how the lifetime of oscillons is sensitive to the amount of asymmetry between the two minima. Here one must be careful to set the initial radius to be smaller than the critical radius, as bubbles with radii larger than critical will grow. As in the symmetric potential case there are no critical bubbles, we can say that we are studying the evolution of subcritical bubbles in symmetric and asymmetric potentials. Oscillons are thus a possible stage in the evolution of subcritical bubbles toward their demise. In Section 6 we discuss several possible situations in which these configurations will play an important rôle. Although we focus mainly on cosmological phase transitions, some of our arguments apply equally well to phase transitions in the laboratory. We conclude in Section 7 with a summary of our results and an outlook to future work.

II. PRELIMINARIES

In this Section we introduce the notation and some definitions which will be useful later on. We also present the exact solution for the evolution of a "Gaussian-shaped" bubble (*i.e.* with $\phi(r, t=0) \sim \exp[-r^2/R^2]$) in the linear regime.

A. General Formalism

The action for a real scalar field in (3+1)-dimensions is

$$S[\phi] = \int d^4x \left[\frac{1}{2}(\partial_\mu\phi)(\partial^\mu\phi) - V_{\mathrm{S(A)}}(\phi)\right] \quad , \tag{1}$$

where the subscripts S and A stand for symmetric (SDWP) and asymmetric (ADWP) double-well potentials, given respectively by,

$$V_{\mathrm{S}}(\phi) = \frac{\lambda}{4}\left(\phi^2 - \frac{m^2}{\lambda}\right)^2 \tag{2}$$

and,

$$V_{\mathrm{A}}(\phi) = \frac{m^2}{2}\phi^2 - \frac{\alpha_0 m}{3}\phi^3 + \frac{\lambda}{4}\phi^4 \quad . \tag{3}$$

Note that the coupling constants λ and α_0 are dimensionless. A solution $\phi(\mathbf{x}, t)$ to the equation of motion,

$$\partial^2\phi/\partial t^2 - \nabla^2\phi = -\frac{\partial V(\phi)}{\partial\phi} \quad , \tag{4}$$

has energy

$$E[\phi] = \int d^3x \left[\frac{1}{2}(\partial\phi/\partial t)^2 + \frac{1}{2}(\nabla\phi)^2 + V(\phi)\right] \quad . \tag{5}$$

We will restrict our investigation to spherically-symmetric configurations. In this case it proves convenient to introduce dimensionless variables, $\rho = rm$, $\tau = tm$, and $\Phi = \frac{\sqrt{\lambda}}{m}\phi$. The nonlinear Klein-Gordon equation is,

$$\frac{\partial^2\Phi}{\partial\tau^2} - \frac{\partial^2\Phi}{\partial\rho^2} - \frac{2}{\rho}\frac{\partial\Phi}{\partial\rho} = \begin{cases} \Phi - \Phi^3 & \text{(SDWP)} \\ -\Phi + \alpha\Phi^2 - \Phi^3 & \text{(ADWP)} \end{cases} \tag{6}$$

where $\alpha = \lambda^{-1/2}\alpha_0$. Note that for the SDWP the two minima are located at $\Phi_0 = -1$ and $\Phi_+ = 1$. For the ADWP (with $\alpha \geq 2$), the minima are at $\Phi_0 = 0$ and $\Phi_+ = \frac{\alpha}{2}\left[1 + \left(1 - \frac{4}{\alpha^2}\right)^{1/2}\right]$. Requiring Φ_+ to be the global minimum implies $\alpha^2 > 9/2$. For $\alpha^2 = 9/2$ the two minima are degenerate with $\Phi_+ = \sqrt{2}$. This value will be important later.

We are interested in following the evolution of unstable spherically-symmetric configurations of initial radius R_0, (from now on we call these initial configurations subcritical bubbles both for the SDWP and the ADWP) which can be thought of as being localized fluctuations about the global vacuum Φ_0. Thus, we must measure the rate at which the initially localized energy is radiated away as the subcritical bubble relaxes to the global vacuum. This can be done by surrounding the initial configuration with a sphere of sufficiently large radius, $R_s \gg R_0$, and measuring the flow of energy through the surface of the sphere. The evolution of subcritical bubbles is obtained by solving the nonlinear Klein-Gordon equation numerically. We define the subcritical bubble's kinetic, surface, and volume energies, respectively, by

$$E_k = 2\pi\int_0^{R_s}\rho^2\dot{\Phi}^2\,d\rho,\ E_s = 2\pi\int_0^{R_s}\rho^2(\Phi')^2\,d\rho,\ E_v = 4\pi\int_0^{R_s}\rho^2 V(\Phi)\,d\rho\ , \tag{7}$$

where a prime denotes derivative with respect to ρ. The bubble's total energy is thus,

$$E_b(\tau) = E_k(\tau) + E_s(\tau) + E_v(\tau)\ . \tag{8}$$

In order to solve the nonlinear Klein-Gordon equation we will impose the following boundary conditions,

$$\Phi(\rho\to\infty,\tau) = \Phi_0,\ \Phi'(0,\tau) = 0,\ \dot{\Phi}(\rho,0) = 0\,. \tag{9}$$

The first condition guarantees that the bubble approaches the vacuum at Φ_0 at spatial infinity. The second condition imposes regularity at the origin, while the last condition states that the bubbles start their evolution at rest. These conditions must be supplemented by the initial profile of the bubble. We will investigate both 'Gaussian' and 'tanh' bubbles which we write as

$$\text{Gaussian: } \Phi(\rho,0)= (\Phi_c - \Phi_0)\, e^{-\rho^2/R_0^2} + \Phi_0 \tag{10}$$

$$\text{tanh: } \Phi(\rho,0)= \frac{1}{2}\left[(\Phi_0 - \Phi_c)\, \tanh(\rho - R_0) + \Phi_0 + \Phi_c\right] \ , \quad R_0 \gg 1 \ . \tag{11}$$

Φ_c is the value of the field at the bubble's core, which we may or not take as being the other minimum of the potential, Φ_+. If we do, the bubble can be interpreted as being a field configuration of initial linear size $\sim 2R_0$ which interpolates between the two vacua. As we will see later, it is not necessary to set $\Phi_c = \Phi_+$ in order to have subcritical bubbles relaxing into oscillons during their evolution. We can now move on to study the evolution of subcritical bubbles in the linear regime.

B. Bubble Evolution in the Linear Regime

As a first application of the above formalism, we will investigate the evolution of Gaussian bubbles in the linear regime. We choose as the linear potential,

$$V_L(\Phi) = (\Phi + 1)^2 \ , \tag{12}$$

as it has a minimum at $\Phi_0 = -1$ with the same curvature as the SDWP. The Klein-Gordon equation has a trivial solution $\Phi(\rho,\tau) = -1$. Separation of variables with a constant $-k^2$ allows us to write $\Phi(\rho,\tau) = -1 + R(\rho)\exp[\pm i\sqrt{k^2+2}\tau]$, with the radial function $R(\rho)$ obeying,

$$R'' + \frac{2}{\rho}R' + k^2 R = 0 \ . \tag{13}$$

This equation has solutions which are linear combinations of $\frac{\sin k\rho}{\rho}$, $\frac{\cos k\rho}{\rho}$. Since $\frac{\cos k\rho}{\rho}$ is singular at the origin we write the general solution as

$$\Phi(\rho,\tau) = -1 + \int_0^\infty dk\, b(k) \frac{\sin k\rho}{\rho} \left[\cos(\sqrt{k^2+2}\,\tau) + a(k)\,\sin(\sqrt{k^2+2}\,\tau)\right] . \qquad (14)$$

The boundary conditions are, writing $\Phi_c \equiv 2q_0 - 1$, q_0 an arbitrary constant,

$$\Phi(\rho,\tau=0) = 2q_0\, e^{-\rho^2/R_0^2} - 1 \qquad (15)$$

$$\Phi(\rho\to\infty,\tau) = -1 \qquad (16)$$

$$\Phi'(\rho=0,\tau) = 0 \qquad (17)$$

$$\dot{\Phi}(\rho,\tau=0) = 0\ . \qquad (18)$$

Eq. 16 is trivially satisfied. Eq. 15 determines $b(k)$,

$$2q_0\, e^{-\rho^2/R_0^2} = \int_0^\infty dk\, b(k) \frac{\sin k\rho}{\rho}\ . \qquad (19)$$

Taking the sine transform we can write,

$$b(k) = \frac{4q_0}{\pi} \mathrm{Im}\left[\int_0^\infty d\rho\, \rho\, e^{-\rho^2/R_0^2} e^{ik\rho}\right] . \qquad (20)$$

The integral can be easily done and we obtain,

$$b(k) = \frac{q_0 R_0^3}{\sqrt{\pi}}\, k\, e^{-R_0^2 k^2/4}\ . \qquad (21)$$

Regularity at the origin is also guaranteed, as $\left[\frac{\sin k\rho}{\rho}\right]'$ vanishes as $\rho \to 0$. Choosing the bubble to start at rest implies that $a(k)$ vanishes. Thus, the final solution satisfying all boundary conditions is,

$$\Phi(\rho,\tau) = -1 + \frac{q_0 R_0^3}{\sqrt{\pi}} \int_0^\infty dk\, k\, e^{-R_0^2 k^2/4}\, \frac{\sin k\rho}{\rho}\, \cos(\sqrt{k^2+2}\,\tau)\,. \qquad (22)$$

In Figure 1 we show a plot of this solution, for initial amplitude $q_0 = 1$ and radius $R_0 = 3$. The bubble performs damped oscillations as it decays into $\Phi_0 = -1$.

It is instructive to investigate the behavior of the bubble's core with time,

$$\Phi(\rho=0,\tau) = -1 + \frac{q_0 R_0^3}{\sqrt{\pi}} \int_0^\infty dk\, k^2\, e^{-R_0^2 k^2/4}\, \cos(\sqrt{k^2+2}\,\tau)\,. \tag{23}$$

The integral is dominated by small values of k, $k \lesssim 2R_0^{-1}$. Thus, we can approximate the argument of $\cos(\sqrt{k^2+2}\tau)$ for $R_0 \gtrsim 2$ and write,

$$\Phi(\rho=0,\tau) = -1 + \frac{q_0 R_0^3}{\sqrt{\pi}} \mathrm{Re}\left[e^{i\sqrt{2}\tau} \int_0^\infty dk\, k^2\, e^{-R_0^2 k^2/4}\, e^{i\sqrt{2}\tau k^2/4}\right] \quad . \tag{24}$$

Performing the integral we obtain

$$\Phi(\rho=0,\tau) = -1 + \frac{2q_0}{(1+2\tau^2/R_0^4)^{3/4}} \cos\left(\sqrt{2}\tau + \frac{3}{2}\tan^{-1}\left(\frac{\sqrt{2}\tau}{R_0^2}\right)\right) \quad . \tag{25}$$

Thus, the amplitude at the core decays as $\tau^{-3/2}$, while the frequency becomes constant for $\tau \gtrsim R_0^2/\sqrt{2}$. The envelope of the core's amplitude decays to $1/e$ of its initial value above $\Phi_0 = -1$ in a time (units restored)

$$t_{1/e} \simeq 1.18 R_0^2 m^{-1}\,. \tag{26}$$

In Fig. 2 we compare the above analytical approximation with the numerical solution of the Klein-Gordon equation (more details later). The excellent agreement gives support to the accuracy of the numerical methods used.

III. EVOLUTION OF SUBCRITICAL BUBBLES IN SDWP: NUMERICAL RESULTS

In this and the next Section we will restrict our analysis to bubbles in SDWP. Section 5 will deal with bubble evolution for ADWPs. The equation of motion is

$$\ddot{\Phi} - \Phi'' - \frac{2}{\rho}\Phi' = \Phi - \Phi^3 \quad , \tag{27}$$

with boundary conditions given by Eqs. 15 – 18. (For tanh bubbles or any other initial bubble profile, just replace Eq. 15 by the appropriate choice.) This equation was solved

numerically using a finite difference scheme fourth order accurate in space and second order accurate in time. The radial dimension of the two-dimensional grid moved outwards with the speed of light in order to avoid any radiation from being reflected on the lattice boundary and thus interfering with the bubble's evolution within the grid (dynamically increasing simulation lattice). The alternative, a sufficiently long but static grid, is extremely time-consuming for long-lived oscillons. The resolution was typically set to $\Delta\rho = 0.1$ and $\Delta\tau = 0.05$; the total energy $E_b + 4\pi \int_{R_s}^{\infty} \rho^2 \left[\frac{1}{2}\dot{\Phi}^2 + \frac{1}{2}(\Phi')^2 + V(\Phi)\right] d\rho$ is then conserved throughout the evolution to better than one part in 10^3. Additionally, high resolution experiments ($\Delta\rho = 0.01$, $\Delta\tau = 0.005$) produced the same results, with an energy conservation of one part in 10^5. We used $R_s = 10$ for the SDWP, and $R_s = 15$ for the ADWP. For reasons that will be made clear soon, we were not interested in bubbles of large initial radius.

Figs. 3a and 3b show the energy of Gaussian and tanh bubbles for several initial radii R_0. (More examples can be found in Ref. [13].) In all the examples we took $\Phi_c = +1$; the bubble interpolates between the two vacua. It is clear that the evolution of the bubbles is very sensitive to the value of R_0. An extensive investigation showed that Gaussian bubbles with $R_0 \lesssim 2.4$ and $R_0 \gtrsim 4.5$ quickly disappear, radiating their initial energies to infinity. However, bubbles with $2.4 \lesssim R_0 \lesssim 4.5$, settle into a period of long-lived stability where practically no energy is radiated away. This stage in their evolution, which we call the oscillon stage, can have a duration approaching $10^3 - 10^4 m^{-1}$, which is remarkably large compared to both short-lived bubbles and to the typical time-scales found for the linear potential. Although the range of values for R_0 which fall into an oscillon stage is sensitive to the initial profile of the configuration, the same results are obtained for other initial bubbles, such as tanh bubbles. This supports our previous claim that oscillons can be viewed as a possible stage during the evolution of subcritical bubbles; after shedding a sufficient fraction of their initial energy, the subcritical bubbles enter the oscillon stage

which is characterized by an energy with a nearly constant value of $\sim 43m/\lambda$, regardless of their initial radius.

The core value of the field, $\Phi(0,\tau)$, performs anharmonic oscillations as shown in Fig. 4a. In Fig. 4b we show a sequence of snapshots of an oscillon. Except when $\Phi(0,\tau) \simeq -1$, an oscillon configuration is very well approximated by a half-Gaussian. We define the effective radius of a localized field configuration by,

$$R_{\rm eff}(\tau) = \frac{\int_0^{R_s} \rho^3 \left[\frac{1}{2}(\Phi')^2 + V(\Phi)\right] d\rho}{\int_0^{R_s} \rho^2 \left[\frac{1}{2}(\Phi')^2 + V(\Phi)\right] d\rho} \quad , \quad R_{\rm eff} \ll R_s \; . \tag{28}$$

In Fig. 5 we show the evolution of this radius for several bubbles during the oscillon stage. The divergence at the end is spurious, signaling that no energy is left within the sphere (the denominator of Eq. 28). It is clear that the effective radius of an oscillon is approximately constant, with variations which are smaller than 20% about a mean of $R_{\rm osc} \simeq 2.8 - 3.0$. This justifies the name given to these configurations: An oscillon is a localized, time-dependent field configuration with nearly constant radius and energy which is characterized by anharmonic oscillations of the field amplitude about the global vacuum.

In order to stress the remarkable longevity of oscillons we show in Figs. 6a and 6b the lifetime as a function of initial radius and energy, respectively. For Gaussian bubbles the longest living oscillon, with $\tau_l \simeq 7.4 \times 10^3$, comes from an initial bubble of radius $R_0 = 2.86$. For tanh bubbles, the longest living oscillon comes from an initial bubble of radius $R_0 = 3.08$, with lifetime $\tau_l \simeq 4.4 \times 10^3$. In Fig. 7 we show the detailed dependence of lifetime as a function of radius for Gaussian bubbles about the peak at $R_0 = 2.86$. (Lifetimes are accurate to within 5%.)

So far we have restricted our investigation to bubbles that interpolate between the two vacua. This is it not a necessary condition for the existence of oscillons although, of course, it is sufficient. As long as the initial value of the field at the bubble's core probes

the nonlinearities of the potential and the initial radius is within the correct range (which varies with initial amplitude), oscillons can exist. We will give an analytical argument for this in the next Section. For now, we will just provide numerical evidence for this fact. In Fig. 8 we show a plot of lifetime for different core values. Clearly, no oscillon can develop if the initial energy is below the plateau energy. Also, we find that no oscillon develops if $\Phi_c \leq \Phi_{\rm inf}$, where $\Phi_{\rm inf} = -1/\sqrt{3}$ is the inflection point closest to Φ_0. Thus, we arrive at the *sufficient conditions* for the existence of oscillons: i) the value of the field at the bubble's core must be above the inflection point, and ii) the initial bubble's energy must be above the plateau energy. Conditions i) and ii) fix the value of R_0 for a given initial bubble to evolve into an oscillon.

This concludes the presentation of our numerical results. In the next Section we will provide semi-analytical arguments to elucidate some of the properties of these configurations.

IV. PROPERTIES OF OSCILLONS

From the results of the previous Sections, it is clear that there are four main questions concerning the oscillons. First, why only bubbles with an initial radius above a certain value develop into oscillons, and how this value depends on the initial amplitude of the field at the bubble's core. Second, why certain oscillons live longer than others. Third, what is the mechanism responsible for the oscillon's final collapse. And finally, why above a maximum initial bubble radius no oscillons are possible. In this Section we address the first three questions. Work on the fourth question is in progress.

In order to treat these questions analytically, we make use of the fact that independently of the initial bubble profile, an oscillon is very well approximated by a half-Gaussian. Even though the Klein-Gordon equation implies that $\Phi(\rho \to \infty, \tau) \sim \exp[-\rho]$,

the difference turns out to be sufficiently small in practice to justify our approximation. In a sense, the tail matters little to the dynamical properties of the configurations. The agreement of our analytical arguments with the numerical results should convince the reader of this fact. We model the oscillon by writing, for the SDWP,

$$\Phi(\rho,\tau) = 2q(\tau)\exp\left[-\rho^2/R^2(\tau)\right] - 1 \quad . \tag{29}$$

With this *ansatz* we have effectively reduced the field theory problem to two degrees of freedom, the amplitude at the core $\Phi_c(\tau) \equiv 2q(\tau) - 1$, and the radius $R(\tau)$. This problem is still quite complicated to treat analytically due to the nonlinear coupling between the two degrees of freedom. Further simplification is guided by the numerical investigation, which showed that the effective radius of the oscillon remains practically constant, with oscillations about its mean value of order 20% or less. Thus, as a first step, we will keep the radius constant, and treat only the amplitude at the core as an effective degree of freedom. Strong as it may seem, this simplification will allow us to extract several important results concerning the observed numerical behavior of these configurations, as we show in the next subsections. We are currently investigating the consequenses of keeping both degrees of freedom $q(\tau)$ and $R(\tau)$.

The above model for the oscillon still misses one important ingredient; it does not include radiation of the bubble's energy to infinity. The justification for neglecting this lies in the fact that oscillons hardly radiate. By excluding radiation it is possible to analytically integrate the energy over the whole space. Using the definitions in Eq. 7 we obtain, for the kinetic, surface and volume energies, respectively,

$$E_k = \frac{\pi\sqrt{2\pi}}{2}R^3\dot{q}^2, \; E_s = \frac{3\pi\sqrt{2\pi}}{2}Rq^2, \; E_v = \pi\sqrt{2\pi}R^3\left(q^2 - \frac{4\sqrt{6}}{9}q^3 + \frac{\sqrt{2}}{4}q^4\right) \quad . \tag{30}$$

A. Existence of Oscillons: Lower Bound on the Initial Radius

From Fig. 6a it is clear that there is a lower bound on the initial value of the bubble radius so that it relaxes into an oscillon during its collapse. Since from our previous discussion we know that oscillons are a product of the nonlinearities in the system, this result suggests that for small enough initial radii the nonlinearities are ineffective to trigger the resonant behavior responsible for the oscillon's longevity. That this is the case can be shown by studying the effective potential controlling the behavior of the amplitude $q(\tau)$. Using the above *ansatz* with constant radius, the energy of the configuration $E = E_k + E_s + E_v$ can be written as the energy of a particle of unit mass with a potential $V(q)$,

$$\frac{E}{16\pi A} = \frac{1}{2}\dot{q}^2 + V(q), \quad V(q) = \left(1 + \frac{B}{A}\right) q^2 - \frac{C}{A}q^3 + \frac{D}{A}q^4 \quad , \tag{31}$$

where $A = \frac{\sqrt{2\pi}}{16}R^3$, $B = \frac{3\sqrt{2\pi}}{32}R$, $C = \frac{\sqrt{3\pi}}{18}R^3$, and $D = \frac{\sqrt{\pi}}{32}R^3$ follow from Eq. 30. The potential V has only one minimum at $q = 0$, ($\Phi = \Phi_0 = -1$, the global vacuum), about which the amplitude performs anharmonic oscillations.

It is the energy localized within a small region surrounding the bubble that may (or not) feed the nonlinear growth of the modes ultimately responsible for the appearance of the oscillon during the collapse of the bubble. This lends further support to the above *ansatz* neglecting radiation. Thus, the equation of motion for the amplitude $q(\tau)$ is,

$$\ddot{q} = -2\left(1 + \frac{B}{A}\right) q + 3\frac{C}{A}q^2 - 4\frac{D}{A}q^3 \quad . \tag{32}$$

Writing $q(\tau) = \bar{q}(\tau) + \delta q(\tau)$, the linearized equation satisfied by the fluctuations $\delta q(\tau)$ is,

$$\ddot{\delta q} = -\omega^2(\bar{q}, R)\delta q, \quad \omega^2(\bar{q}, R) \equiv 3\sqrt{2}\bar{q}^2 - 8\frac{\sqrt{6}}{3}\bar{q} + \left(2 + \frac{3}{R^2}\right) \quad , \tag{33}$$

where we have substituted the numerical values of the constants A, B, C, and D in the expression for the frequencies $\omega^2(\bar{q}, R)$. Note that $\omega^2(\bar{q}, R)$ is simply the curvature of the

potential dictating the dynamics of the amplitude $q(\tau)$. As the bubble radiates its energy away, the configuration decays into the vacuum. However, for $\omega^2(\bar{q}, R) < 0$, fluctuations about $\bar{q}$ are unstable, driving the amplitude away from its vacuum value. These are the fluctuations which are mainly responsible for the appearance of the oscillon. In Fig. 9 we show a plot of the surface $\omega^2(\bar{q}, R)$. It has one minimum at $\bar{q}_{\rm min} \simeq 0.77$ (with location independent of R!), where its value is $\omega^2(q_{\rm min}, R) \simeq -0.514 + 3R^{-2}$. Thus, only for $R > R_{\rm min} \simeq 2.42$, $\omega^2 < 0$ and fluctuations can grow. In other words, *only for* $R_0 > R_{\rm min} \simeq 2.42$ *are oscillons possible.* This lower bound on the value of the radius agrees very well with our numerical results (see Fig. 6a). It is independent of the initial amplitude of the bubble. All bubbles with initial radius smaller than $R_{\rm min}$ will quickly collapse. (For core amplitudes above $\Phi_c = 1$, it is possible to decrease the initial radius by about 20% or so and still obtain oscillons.)

B. Collapse of Oscillons

The above analysis can also provide information about the final decay of oscillons. For $R > R_{\rm min}$, $\omega^2(\bar{q}, R)$ will be negative for amplitudes,

$$\bar{q}_- \leq \bar{q} \leq \bar{q}_+ , \quad \bar{q}_\pm = \frac{4\sqrt{3}}{9}\left[1 \pm \left(1 - \frac{9\sqrt{2}}{16}\left(1 + \frac{3}{2R^2}\right)\right)^{1/2}\right] . \tag{34}$$

Thus, for $R > R_{\rm min}$ there is a minimum value for the amplitude at the core, shown in Fig. 10, $\Phi_c^-(R) = 2\bar{q}_-(R) - 1$, below which the oscillon slips into the linear regime and quickly decays. This result can be understood as follows: As the bubble settles into the oscillon configuration with energy given by the plateau energy $E \sim 43m/\lambda$ and radius $R_{\rm eff} \sim 2.8m^{-1}$, there is a maximum value for the amplitude of the field at the core. This value is obtained from the formula for the static energy with its value fixed at the plateau value and with radius $R \simeq R_{\rm eff}$, and it is $\Phi_c \sim 0.2$. The values of the field at the oscillon's core obtained numerically are always marginally within the allowed region

which gives $\omega^2 < 0$; the oscillon survives while fluctuations are unstable. However, during the oscillon stage, energy is slowly being radiated away, and thus the amplitude at the core is slowly decreasing while the average value of the radius is slowly increasing (Fig. 5). From Fig. 10 and the argument above, below a certain value for the amplitude at the core the perturbations enter the linear regime and the oscillon decays. A comparison between $\Phi_c^-(R_{\rm eff})$ and the numerical values of the core's amplitude at the last oscillation is given in Table 1. In interpreting these results, we must keep in mind the crudeness of the analytical approximation used to obtain $\Phi_c^-(R)$. Even so, at least for the longest living oscillons, it is clear that during the last oscillation the amplitude falls below $\Phi_c^-(R)$. A more detailed analysis shows that the amplitude falls below $\Phi_c^-(R)$ during the last few oscillations, as the configuration starts to approach the linear regime responsible for its final demise. For completeness, in Fig. 11 we show a phase-space portrait of the evolution of $\Phi_c(\tau)$ during the oscillon stage and its final collapse, for a bubble with initial radius $R_0 = 3.0$. Clearly, the final spiraling into $\Phi_0 = -1$, typical of the linear regime, occurs as the maximum core amplitude (for $\dot{\Phi} = 0$) falls roughly below Φ_c^-.

C. Lifetime of Oscillons

A question which is of great interest is the determination of the oscillon's lifetime as a function of the bubble's initial radius and core value. Although we were unable to obtain an analytical expression for the lifetime, we do understand why some oscillons live longer than others. Our argument is based on the virial theorem for spherically-symmetric scalar field configurations, which we derive next.

Multiplication of the equation of motion, $\partial^2\phi/\partial t^2 - \partial^2\phi/\partial r^2 - (2/r)\,\partial\phi/\partial r = -\frac{\partial V(\phi)}{\partial\phi}$ (cf. Eq. 4), by $4\pi r^2\phi$ and integrating over r gives, after integration by parts,

$$4\pi\int_0^\infty r^2\phi\ddot{\phi}\,dr + 4\pi\int_0^\infty r^2\phi'^2\,dr + 4\pi\int_0^\infty r^2\phi\frac{\partial V}{\partial\phi}\,dr = 0 \quad , \qquad (35)$$

where we assumed that $\lim_{r\to\infty} r^2\phi' = 0$. The second term is easily recognized as twice the total surface energy. Performing a time averaging over one period, denoted by

$$\langle\ \rangle \equiv \frac{1}{T}\int_T dt \tag{36}$$

we get

$$\frac{4\pi}{T}\int_0^\infty r^2\,dr\int_T dt\dot{\phi}\ddot{\phi}\ + 2\langle E_s\rangle + 4\pi\left\langle\int_0^\infty r^2\phi\frac{\partial V}{\partial\phi}\,dr\right\rangle = 0 \tag{37}$$

and after integrating by parts the time integral in the first term, (the boundary term $\phi\dot{\phi}$ vanishes due to the integration over a period),

$$-\frac{1}{T}\int_T dt\,4\pi\int_0^\infty r^2\dot{\phi}^2\,dr + 2\langle E_s\rangle + 4\pi\left\langle\int_0^\infty r^2\phi\frac{\partial V}{\partial\phi}\,dr\right\rangle = 0\ \ . \tag{38}$$

Identifying the first term as twice the time-averaged kinetic energy, we arrive at the virial theorem

$$\langle E_k\rangle = \langle E_s\rangle + 2\pi\left\langle\int_0^\infty r^2\phi\frac{\partial V}{\partial\phi}\,dr\right\rangle\ \ . \tag{39}$$

For the SDWP, in dimensionless variables,

$$\langle E_k\rangle = \langle E_s\rangle + 2\pi\left\langle\int_0^\infty \rho^2\Phi^2(\Phi^2-1)\,d\rho\right\rangle . \tag{40}$$

As usual, the virial theorem holds as an equality only for strictly periodic systems. Numerical simulations of oscillons show, however, that the basic oscillation is overlaid by a long-wavelength modulation and other deviations from strict periodicity. It is hence of interest to analyze the "departure from virialization",

$$\mathcal{V}(\tau) \equiv \langle E_k\rangle - \langle E_s\rangle - 2\pi\left\langle\int_0^{R_*} \rho^2\Phi^2(\Phi^2-1)\,d\rho\right\rangle , \tag{41}$$

where now

$$E_k = 2\pi\int_0^{R_*}\rho^2\dot{\Phi}^2\,d\rho,\ E_s = 2\pi\int_0^{R_*}\rho^2(\Phi')^2\,d\rho \tag{42}$$

and $R_s \approx 10$ as before is an integration cut-off large enough to encompass the entire configuration. For a perfectly virialized configuration, $\mathcal{V}(t) = 0$. In Fig. 12 we show the evolution of $\mathcal{V}$ for several Gaussian bubbles. When contrasted with Fig. 6a, it becomes clear that *the longer the lifetime of the oscillon, the better virialized it is.* This result is made more transparent by plotting the lifetime as a function of the maximum value of $\mathcal{V}$ for several radii, as shown in Fig. 13. Note also the symmetry about the longest-living oscillon, with $R_0 = 2.86$.

Using the virial relation and the numerical results, we can obtain a semi-analytical estimate for the optimal radius for an oscillon, that is, the one which is longest-lived. Although we perform the calculation for the SDWP, our methods can be easily generalized for any potential. With the *ansatz* for the Gaussian profile given in Eq. 29, the time-averaged oscillon energy, and the departure from virialization, $\mathcal{V}$, are, respectively,

$$\frac{\langle E \rangle}{\pi^{3/2}} = \left(\frac{\sqrt{2}}{2}\langle \dot{q}^2 \rangle + \sqrt{2}\langle q^2 \rangle - \frac{8\sqrt{3}}{9}\langle q^3 \rangle + \frac{1}{2}\langle q^4 \rangle \right) R^3 + \frac{3\sqrt{2}}{2}\langle q^2 \rangle R \, , \tag{43}$$

and

$$\frac{\mathcal{V}}{\pi^{3/2}} = \left(\frac{\sqrt{2}}{2}\langle \dot{q}^2 \rangle + 2\langle q \rangle - \frac{5\sqrt{2}}{2}\langle q^2 \rangle + \frac{16\sqrt{3}}{9}\langle q^3 \rangle - \langle q^4 \rangle \right) R^3 - \frac{3\sqrt{2}}{2}\langle q^2 \rangle R \ . \tag{44}$$

Multiplying the expression for the time-averaged energy by 2 we can eliminate the cubic and quartic terms in the expression for $\mathcal{V}$. Using that for the longest-lived oscillon $\mathcal{V} \simeq 0$, we obtain a cubic equation for the optimal radius, $R_{\rm max}$,

$$\left(\frac{3\sqrt{2}}{2}\langle \dot{q}^2 \rangle - \frac{\sqrt{2}}{2}\langle q^2 \rangle + 2\langle q \rangle \right) R_{\rm max}^3 + \frac{3\sqrt{2}}{2}\langle q^2 \rangle R_{\rm max} - 2\pi^{-3/2}\langle E \rangle \simeq 0 \ . \tag{45}$$

To proceed, we further assume that $q(\tau)$ is periodic, which is a good approximation for the longest-lived oscillon. Writing $q(\tau) = q_0 \cos(\omega\tau)$, with q_0 an amplitude determined numerically (the reader should be careful to distinguish between this ω and the one used in the linear perturbation analysis), the time-averaging can be performed and we finally obtain,

$$\frac{\sqrt{2}}{4}\left(3\omega^2-1\right)q_0^2R_{\max}^3+\frac{3\sqrt{2}}{4}q_0^2R_{\max}-2\pi^{-3/2}\langle E\rangle\approx 0\ . \tag{46}$$

The roots of this equation are determined once we know the values of the parameters $\langle E\rangle$, q_0, and ω. These can be obtained numerically using the remarkable independence of oscillons on initial conditions. We use $\langle E\rangle \simeq 43$, and $\omega = 2\pi/T \simeq 1.37$. The maximum core amplitude, Φ_c, is roughly bounded by $-0.1 \lesssim \Phi_c \lesssim 0.2$, which gives for q_0 the range $0.45 \lesssim q_0 \lesssim 0.6$. With these parameters, we find that the equation has only one real root, bounded by $2.90 \lesssim R_{\max} \lesssim 3.54$. This range of values is in excellent agreement with the observed numerical range for the oscillon radius (see Fig. 5) providing strong support to our arguments. It also gives the correct range of initial values for the radius of bubbles which will relax into the longest-lived oscillons. Thus, the oscillon can be interpreted as the attractor field configuration which minimizes the departure from virialization.

V. EVOLUTION OF SUBCRITICAL BUBBLES IN ADWP: NUMERICAL RESULTS

It was first noted in Ref. [13] that oscillons will also be present for nondegenerate potentials. Most of the analytical arguments above will also apply in this case. In particular, the minimum radius for subcritical bubbles to evolve into oscillons can also be obtained by the perturbation analysis presented in Section 4.A. The sufficient conditions for the existence of oscillons will still be the same, namely, that the initial energy be above the plateau energy, and that the initial core amplitude be above the inflection point of the potential. Of course, the plateau energy will depend on the degree of asymmetry of the potential. The important difference is that for ADWPs, the $O(3)$-symmetric equations of motion admit static solutions known as bounces [16]. These are the well-known critical bubbles of strong first order phase transitions, which specify the thermal barrier for the decay of metastable states, $E_{\rm crit}$ [17]; bubbles with radii larger than critical will grow,

converting the metastable phase into the stable phase with lower free-energy density. Thus, when discussing oscillons in the context of ADWPs, we must make sure that the initial configurations have radii smaller than the critical bubble radius, $R_{\rm crit}$, as well as energies smaller than the decay barrier. The initial bubble energy is bounded by the plateau energy from below and the decay barrier from above.

In order to see the effects of the asymmetry on the properties of the oscillons, we start by showing the results for the degenerate case, obtained by setting $\alpha = 3/\sqrt{2}$ in Eq. 6. Recall that in this case the minima are at $\Phi_0 = 0$ and $\Phi_+ = \sqrt{2}$. In Fig. 14 we show the lifetime of oscillons as a function of initial radius for several core amplitudes. Note that the lifetimes are larger than for the SDWP (Fig. 6a). This is simply due to the fact that for $\alpha = 3/\sqrt{2}$ the ADWP is shallower and narrower than the SDWP, softening the surface energy of the initial bubbles. In Fig. 15a we show the lifetimes vs. radii of initial Gaussian bubbles leading to long-lived oscillons for different values of α. For reference we also show the values of the critical radii. The perturbative analysis of Section 4.A can easily be adapted to this ADWP case, yielding an expression for the frequencies $\omega^2(\bar{q}, R)$ of small fluctuations (analogous to Eq. 33),

$$\omega^2(\bar{q}, R) \equiv \frac{3\sqrt{2}}{4}\bar{q}^2 - \frac{4\sqrt{6}\alpha}{9}\bar{q} + \left(1 + \frac{3}{R^2}\right) \quad . \tag{47}$$

The minimum of this surface (for fixed α) is once again independent of R with $\bar{q}_{\rm min} \simeq 0.51\alpha$, hence oscillons are possible only for $R_0 > R_{\rm min} \simeq (3/(0.28\alpha^2 - 1))^{1/2}$. With the values $\alpha = 3/\sqrt{2}$, 2.16 and 2.23 we then obtain $R_0 > 3.39$, 3.12 and 2.76 respectively, results which compare favorably with the numerical simulation values of $R_0 > 3.2$, 3.1 and 2.9, respectively. In Fig. 15b we show lifetime vs. initial bubble energy for different values of α. For reference we give the values of the plateau energy and of the decay barrier. Note that as the asymmetry is increased, the lifetimes of the oscillons also increase, almost by a factor of two between the nearly degenerate $\alpha = 2.16$ and the more

asymmetric $\alpha = 2.23$, while the ratio between the critical bubble radius, $R_{\rm crit}$, and the longest-lived oscillon, $R_{\rm max}$, varies from $R_{\rm crit}/R_{\rm max} \simeq 5$ for $\alpha = 2.16$ to $R_{\rm crit}/R_{\rm max} \simeq 2$ for $\alpha = 2.23$. As the asymmetry is increased, the oscillons approach more and more the critical bubble, explaining their increased longevity.

VI. OSCILLONS IN ACTION: POSSIBLE APPLICATIONS

In this Section we will present a few situations in which we expect oscillons to be relevant. As we will argue below, their remarkable longevity makes them specially interesting in the context of phase transitions; if thermally nucleated, their presence can affect the dynamics of the transition in several ways. It is not our intention here to give a detailed treatment of the rôle of oscillons on the dynamics of phase transitions, but simply to stress the interesting physics that can emerge due to these configurations.

As we have seen, a typical range of lifetimes is between $t_l = 10^3 - 10^4\ m^{-1}$ in units of the mass m introduced in Eqs. 2 and 3. This is much longer than that of the solution to the spherically symmetric linear Klein-Gordon equation $\sim 5m^{-1}$. The expansion rate of the Universe in a radiation-dominated regime can be written in terms of the background temperature T as $H^2 \propto T^4/m_{\rm Pl}^2$, where H is Hubble's parameter. Thus, the expansion time-scale is $t_U \sim H^{-1} \propto (m_{\rm Pl}/T)T^{-1}$. Typically, the symmetry breaking temperature T_c can be written in terms of the mass scale m of the theory as $T_c \simeq m/\sqrt{\lambda}$. Thus, the expansion time-scale at T_c is $t_U \sim \lambda(m_{\rm Pl}/m)m^{-1}$. The ratio between the oscillon lifetime (taking $t_l = 10^4\ m^{-1}$) and the expansion time-scale is then, $t_l/t_U \sim \lambda^{-1}10^4(m/m_{\rm Pl})$. From this we see that for masses of order the GUT scale the lifetime of the oscillons is comparable (or larger, for weak coupling!) to the age of the Universe at that scale, an intriguing possibility. In such a scenario these unstable field configurations could have a dramatic effect on the dynamics of any phase transition. For example, during a first

order phase transition those subcritical bubbles which go on to form oscillons could last long enough to become critical bubbles as the Universe cooled. In this way we would have a method of completing the transition quicker. Another possibility is that oscillons act as seeds or nucleation sites for the critical bubbles. The combination of these two effects will increase the production rate of critical bubbles, a feature which may well have useful consequences for the old inflationary universe scenario. That model failed partly because the production rate of critical sized bubbles and larger could not keep pace with the exponential expansion of the Universe. If the bubble nucleation rate were increased, then this problem may well be overcome.

For oscillons to be relevant cosmologically, not only must they survive for long enough, they must be thermally produced in large enough numbers since they are unstable and eventually decay. A naive estimate of this rate is that the number density of oscillons of size R produced at temperature T due to thermal fluctuations is

$$n(R,T) \sim T^3 e^{-F(R)/T} ,$$

where $F(R)$ is the free-energy of the configuration of radius R and is given by $F(R) = E_s + E_v$ in Eq. 30. Comparing $F(R_{osc})$ with $F(R_{cr})$ gives an indication of the fraction of bubbles which are oscillons as opposed to critical at any given temperature T. In fact we can see quite easily that although the oscillons are unstable they are produced in much greater abundance, as their free-energy barrier is typically smaller than that for critical bubbles. To be sure of this we require that their thermal nucleation rate be considerably larger than the expansion rate of the Universe, *i.e.* $\Gamma_{\rm th}(R,T)/H \gg 1$. Since $H \propto T^2/m_{\rm Pl}$, it becomes a straightforward comparison. For the case of the electroweak transition, Gleiser and Kolb [9] have shown that the condition on subcritical bubbles can be written as $F(R)/T < 34$. This in turn imposes a constraint on the mass of the associated Higgs, which turns out to be $m_{\rm Higgs} \geq 88$GeV (see [18] for details). It seems

to be the case that oscillons will have an important effect on the dynamics of sufficiently weak first order phase transitions.

In this paper we have been investigating the existence of oscillons for both first and second order phase transitions. A number of issues arise common to both cases which require further study. The first concerns the coupling of oscillons to other forms of matter, whether they be other scalar fields, gauge fields or fermions. We have regarded the oscillons as emerging from an effective theory in which the fields to which it is coupled have been integrated out (a procedure we would hope is valid for low enough energies), leaving an effective potential for the scalar field. Ideally we would like to consider the full theory and solve for all the fields without integrating out the massive ones. It could be that one of these fields leads to an instability in the Φ field which causes the oscillon to decay faster than we have estimated. On the other hand, coupling the oscillon to a charged field may enhance its lifetime, as in the case of nontopological solitons [4]. A second issue concerns the coupling of oscillons to hot plasmas, as would be the case during thermal phase transitions. The plasma would act both as a viscous medium and as an enhancer of fluctuations, presumably affecting the lifetime of the oscillons. We are currently investigating both issues.

The discussion in this Section has concentrated on early Universe aspects of oscillons. Since they are field theories we should expect them to be seen at laboratory energies as well. This may not be so easy to do in practice, but there are many examples of phase transitions in liquid crystals and Ising-like systems which produce nonlinear field theory objects such as topological defects [19]. Also, solutions to the nonlinear Schrödinger equation have been known to be of importance in several contexts, including the propagation of information in optical fibres [20]. It is reasonable to expect that oscillons will be present in the non-relativistic limit, thus being possible solutions to the time-dependent nonlinear Schrödinger equation as well. What would be required for oscillons is a distinct

signature. It could be that as the energy of the system reaches its plateau during the oscillon stage, the material has a particular refractive index and thus could be detected in scattering experiments.

VII. CONCLUSIONS AND OUTLOOK

In this paper we have presented the results of a detailed investigation of the properties of oscillon configurations and explained, where possible, the physics behind their interesting dynamics. The fact that they exist in both first and second order phase transitions makes them of particular interest. They are localized, non-singular, time-dependent, spherically-symmetric solutions of nonlinear scalar field theories, which are unstable but extremely long-lived, with lifetimes of order $10^3 - 10^4\ m^{-1}$, where m is the mass of the scalar field. They naturally appear during the collapse of spherically symmetric field configurations. We have obtained the conditions required for their existence, namely that the initial energy needs to be above a plateau energy and the initial amplitude of the field needs to be above the inflection point on the potential in order to probe the nonlinearities of the theory (but does not need to be at the true minimum of the potential).

Of the many intriguing aspects of these configurations, some that stand out include the fact that they exist only for a given range of initial radii and core amplitudes. The lower value of the radii can be explained by perturbation theory. It corresponds to the minimum radius beyond which the field probes the nonlinearity of the potential. Explaining the upper bound for the initial radius of the field profile is not so straightforward and we are currently investigating this. It could well be that since larger bubbles have larger initial energies, during their collapse higher nonspherical modes are excited, triggering the rapid growth of instabilities responsible for the bubble's collapse before it can settle into the oscillon stage. Another remarkable feature is that the plateau energy of the

oscillon is practically independent of the initial radius. We have interpreted this fact by showing that the oscillon can be thought of as the attractor field configuration which minimizes the departure from virialization.

There is much that remains to be investigated. One concern is that we only investigated stability to radial perturbations. We really need to investigate how nonspherical perturbations affect the spherically symmetric solutions. One possibility is that they will tend to make the oscillons collapse into a pancake configuration, and hence decay more quickly than in the spherical case, although we believe this will only be the case for bubbles with large initial radii. We may also think of higher nonspherical modes as excited states of the "ground-state" $\ell = 0$ resonance studied here. It is thus possible that oscillons may appear in higher energy configurations, which may decay either to the ground-state oscillon or just into scalar radiation. Finally, a more detailed study of the coupling of these objects to other matter fields and hot plasmas is required in order to investigate how they affect the dynamics of phase transitions and how their own decay is affected by these couplings. It is clear though that they are of interest cosmologically. We are currently analyzing the consequences of oscillons if they were to be formed at the electroweak scale [18].

ACKNOWLEDGMENTS

We thank Tanmay Vachaspati for stimulating discussion during the early stages of this work. This collaboration was partially supported by a NATO Collaborative Research Grant 'Cosmological Phase Transitions' no. SA-5-2-05 (CRG 930904) 1082/93/JARC-501. EJC was supported by PPARC and would like to thank the Isaac Newton Institute where part of this work was completed for financial support and their kind hospitality. MG thanks the School of Mathematical and Physical Sciences of the University of Sussex

and the Nasa/Fermilab Astrophysics Center for their kind hospitality, where part of this work was completed. At Fermilab MG was partially supported by NASA Grant NAG 5-2788 and DOE. MG was partially supported by the National Science Foundation through a Presidential Faculty Fellows Award no. PHY-9453431, and by Grant no. PHYS-9204726. He also acknowledges support from NASA Grant NAGW-4270. HRM thanks Dartmouth College for a Graduate Fellowship.

REFERENCES

1. For reviews see, A. C. Scott, F. Y. F. Chiu, and D. W. Mclaughlin, Proc. IEEE **61** (1973) 1443; S. Coleman, *Aspects of Symmetry* (Cambridge University Press, Cambridge, 1985).

2. G. H. Derrick, J. Math. Phys. **5**, 1252 (1964).

3. R. Rajaraman, *Solitons and Instantons* (North-Holland, Amsterdam, 1987).

4. T.D. Lee and G.C. Wick, Phys. Rev. **D9**, 2291 (1974); R. Friedberg, T. D. Lee, and A. Sirlin, Phys. Rev. **D13**, 2739 (1976); *ibid.* **D13**, 2379 (1976); E. Copeland, E.W. Kolb, and K. Lee, Nucl. Phys. **B319**, 501 (1989).

5. J. Frieman, G. Gelmini, M. Gleiser, and E. W. Kolb, Phys. Rev. Lett. **60**, 2101 (1988); J. Frieman, M. Gleiser, A. Olinto, and C. Alcock, Phys. Rev. **D40**, 3241 (1989); R. Friedberg, T. D. Lee, and Y. Pang, Phys. Rev. **D35**, 3658 (1987), and references therein. Recently, the possibility of pseudostable axion breathers has been advanced by E. W. Kolb and I. Tkachev, Phys. Rev. **D49**, 5040 (1994).

6. S. Coleman, Nucl. Phys. **B262**, 263 (1985); A. M. Safian, S. Coleman, and M. Axenides, *ibid.* **B297**, 498 (1988).

7. For reviews see, A. Vilenkin and E.P.S. Shellard, *Cosmic Strings and other Topological Defects* (Cambridge: CUP. 1994); M.B. Hindmarsh and T.W.B. Kibble, *Cosmic Strings*, submitted to Rep. Prog. Phys. (hep-ph/9411342).

8. M. Gleiser, E. W. Kolb, and R. Watkins, Nucl. Phys. **B364**, 411 (1991).

9. M. Gleiser and E. W. Kolb, Phys. Rev. Lett. **69**, 1304 (1992).

10. M. Dine, R. Leigh, P. Huet, A. Linde, and D. Linde, Phys. Rev. **D46**, 550 (1992); G. Anderson, Phys. Lett. **295B**, 32 (1992).

11. G. Gelmini and M. Gleiser, Nucl. Phys. **B419**, 129 (1994) (hep-ph/9211303).

12. I. L. Bogolubsky and V. G. Makhankov, Pis'ma Zh. Eksp. Teor. Fiz. **24**, 15 (1976) [JETP Lett., **24**, 12 (1976)]; *ibid.* **25**, 120 (1977) [*ibid.* **25**, 107 (1977)]; V. G. Makhankov, Phys. Rep. **C 35**, 1 (1978).

13. M. Gleiser, Phys. Rev. **D49**, 2978 (1994) (hep-ph/9308279).

14. D.K. Campbell, J. F. Schonfeld, and C.A. Wingate, Physica **9D**, 1 (1983).

15. I. L. Bogolubsky, Phys. Lett. **A61**, 205 (1977); J. Geicke, Phys. Scripta **29**, 431 (1984); B. A. Malomed and E. M. Maslov, Phys. Lett. **A160**, 233 (1991); A. M. Srivastava, Phys. Rev. **D46**, 1353 (1992); E. M. Maslov, Phys. Lett. **A151**, 47 (1990).

16. S. Coleman, Phys. Rev. **D15**, 2929 (1977); C. Callan and S. Coleman, Phys. Rev. **D16**, 1762 (1977).

17. A. D. Linde, Phys. Lett. **70B**, 306 (1977); Nucl. Phys. **B216**, 421 (1983); [Erratum: **B223**, 544 (1983)].

18. E. J. Copeland, M. Gleiser, and H.-R. Müller, in progress.

19. I. Chuang, R. Durrer, N. Turok and B. Yurke, Science. **251**, 1336 (1991).

20. A. Kumar in *Solitons: Introduction and Applications*, Ed. M. Lakshmanan (Springer-Verlag, Berlin, 1988)

List of Figures

Figure 4b. Snapshots of oscillon with initial radius $R_0 = 2.5$. The snapshots are $\Delta\tau = 0.2$ apart. The dotted lines are snapshots with $\dot{\Phi} > 0$ for $\tau > 504$.

Figure 5. Evolution of averaged oscillon radius for several initial Gaussian bubbles.

Figure 6a. Oscillon lifetime vs. initial radius of Gaussian and tanh bubbles (SDWP).

Figure 6b. Oscillon lifetime vs. initial bubble energy.

Figure 7. Detail of oscillons' lifetime around the peak.

Figure 8a, b. Oscillon lifetime vs. initial Gaussian radius and vs. initial energy, respectively, for different initial core amplitudes.

Figure 9. The frequency surface $\omega^2(\bar{q}, R)$.

Figure 10. Minimum amplitude Φ_c^- for nonlinear growth vs. radius.

Figure 11. Phase-space portrait of an oscillon for $R_0 = 3.0$. The sampling occured every $\Delta\tau = 1.0$.

Figure 12. Departure from virialization vs. time for several initial bubble radii.

Figure 13. Oscillon lifetime vs. maximum value for departure from virialization for several initial radii.

Figure 14. Oscillon lifetime vs. radius for several initial core values with $\alpha = 3/\sqrt{2}$.

Figure 15a. Oscillon lifetime vs. initial radius for several values of α. The respective values of the critical bubble radius are also shown.

Figure 15b. Oscillon lifetime vs. initial energy for several values of α. The respective values of the oscillon's plateau energy and of the decay energy barrier are also shown.

List of Tables

Table 1. Comparison between analytical value for core amplitude appropriate for oscillon stability (Eq. 34) and numerical value of core's amplitude at last oscillation for several oscillons. The value of the radius used in analytical formula was obtained numerically

(see Fig. 5).

TABLE 1

R_0	Range of $R_{\rm eff}$	Range of Φ_c^-	$\Phi_{c,\ \rm num}$
2.4	2.635 – 3.737	0.00836 – 0.2614	0.2705
2.5	2.781 – 3.563	0.0278 – 0.1946	0.1626
2.6	2.893 – 3.532	0.0316 – 0.1564	0.09160
2.7	3.010 – 3.458	0.0413 – 0.1242	0.02574
2.8	3.159 – 3.298	0.0656 – 0.09091	0.05090
2.9	3.120 – 3.333	0.0599 – 0.09892	0.03163
3.0	2.991 – 3.403	0.0492 – 0.1290	0.03631
3.1	2.904 – 3.439	0.0440 – 0.1531	0.08632
3.3	2.778 – 3.575	0.0263 – 0.1957	0.1640
3.5	2.680 – 3.575	0.0263 – 0.2380	0.2368
3.7	2.589 – 3.848	0.0237 – 0.2890	0.3113

FIGURE 1

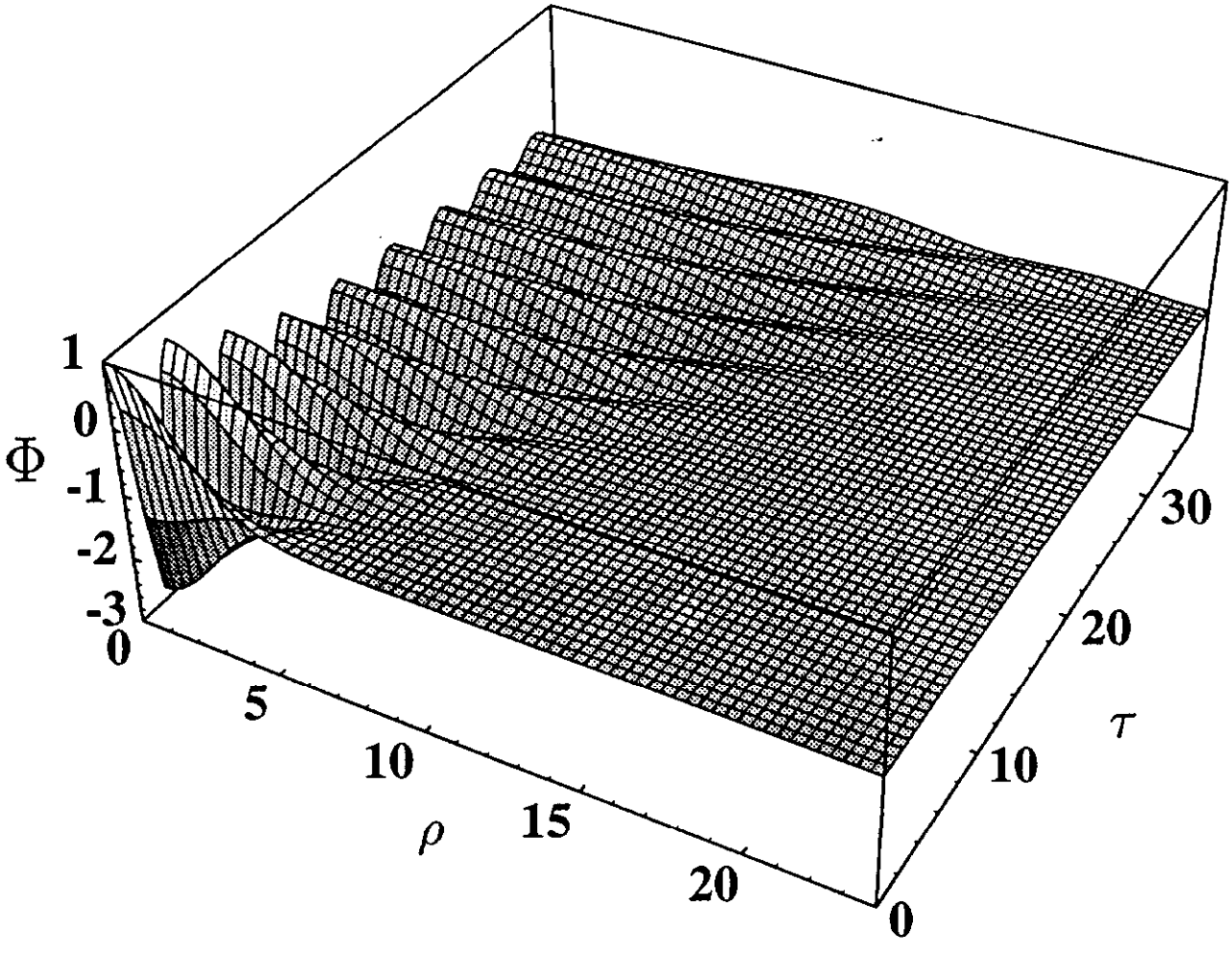

FIGURE 2

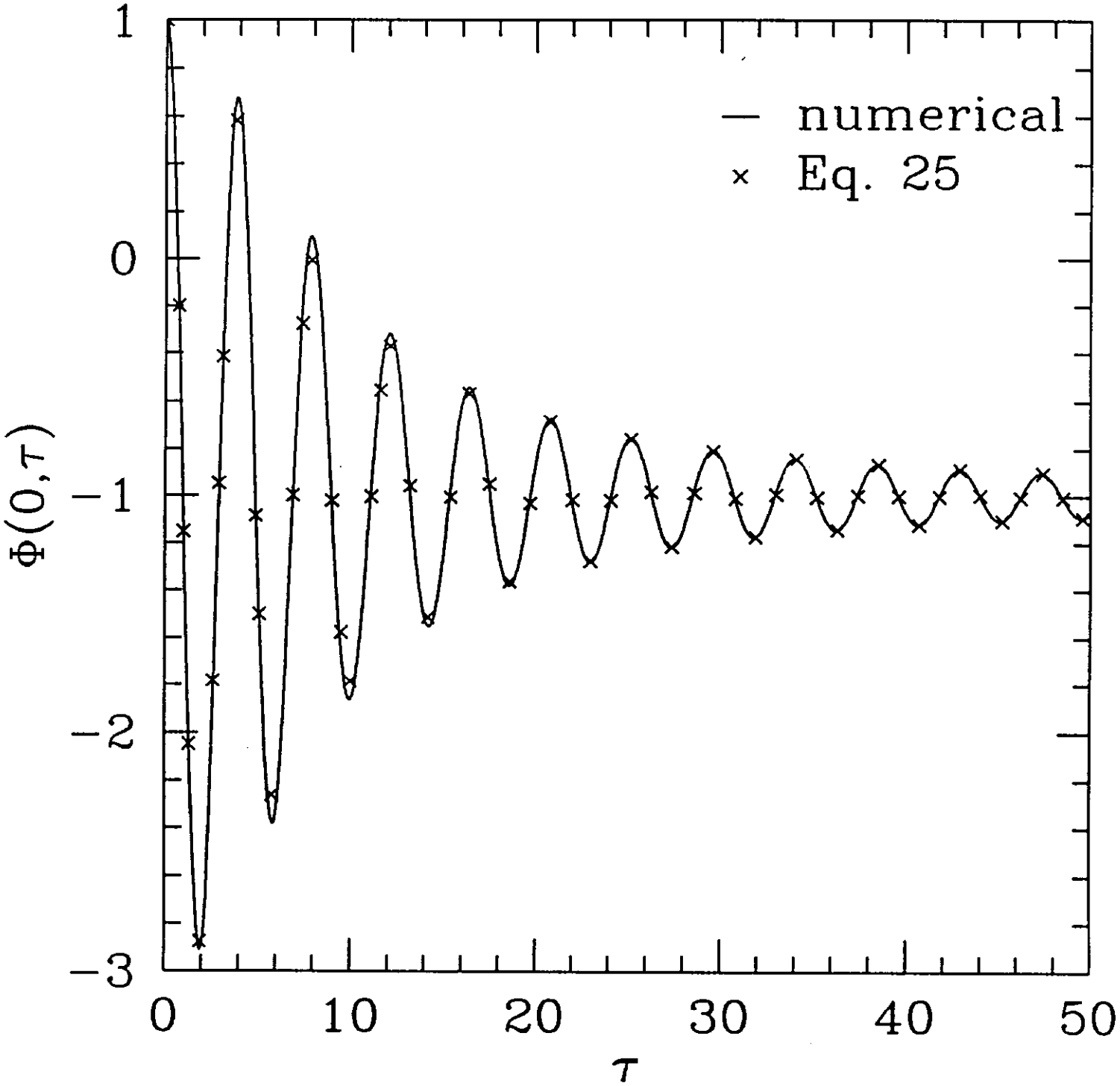

FIGURE 3a

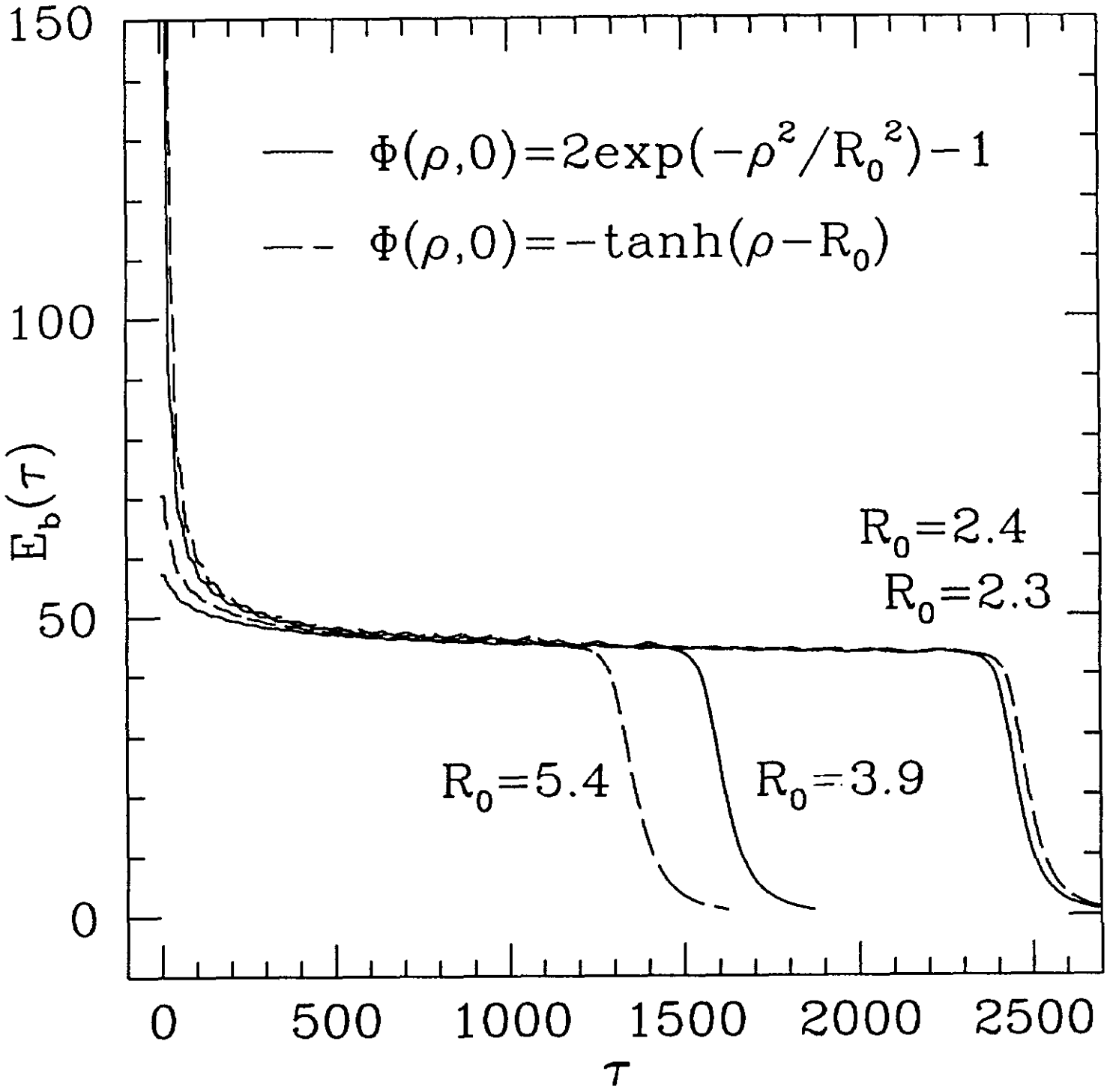
150
100
50
0
$E_b(\tau)$
$\Phi(\rho,0)=2\exp(-\rho^2/R_0^2)-1$
$\Phi(\rho,0)=-\tanh(\rho-R_0)$
$R_0=2.4$
$R_0=2.3$
$R_0=5.4$
$R_0=3.9$
0
500
1000
1500
2000
2500
τ

FIGURE 3b

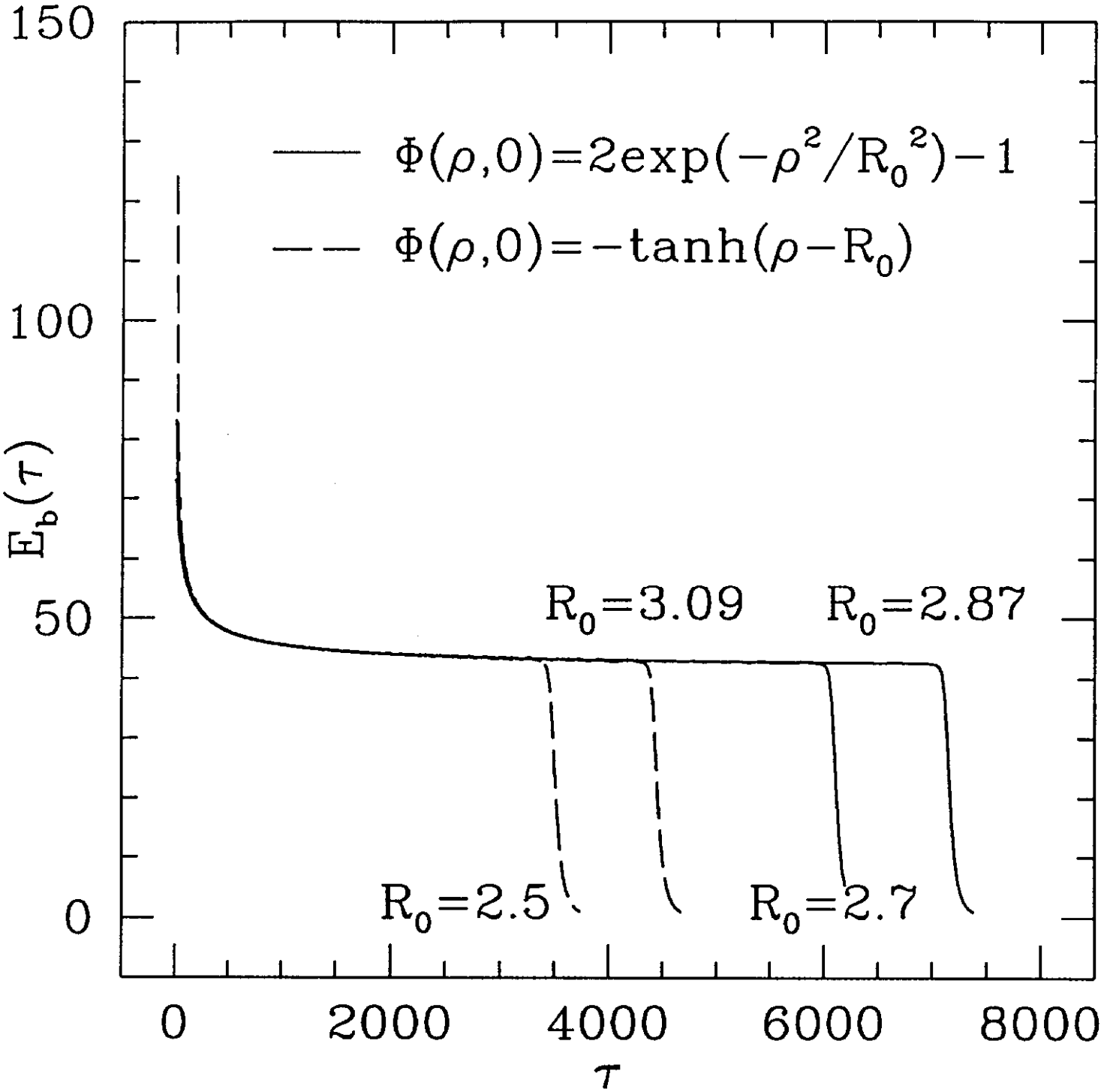
150
100
50
0
$E_b(\tau)$
$\Phi(\rho,0)=2\exp(-\rho^2/R_0^2)-1$
$\Phi(\rho,0)=-\tanh(\rho-R_0)$
$R_0=3.09$
$R_0=2.87$
$R_0=2.5$
$R_0=2.7$
0
2000
4000
6000
8000
τ

FIGURE 4a

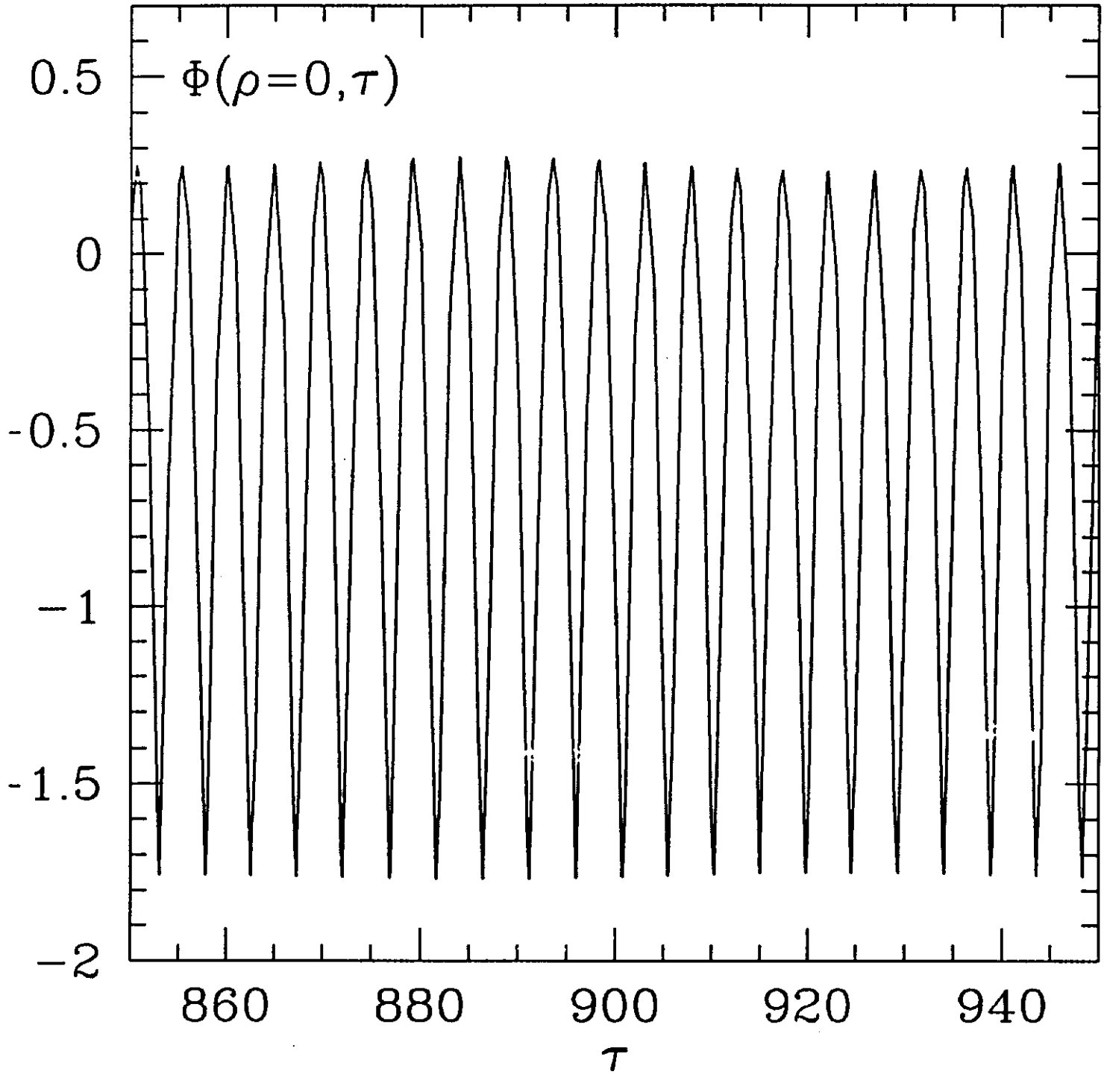

FIGURE 4b

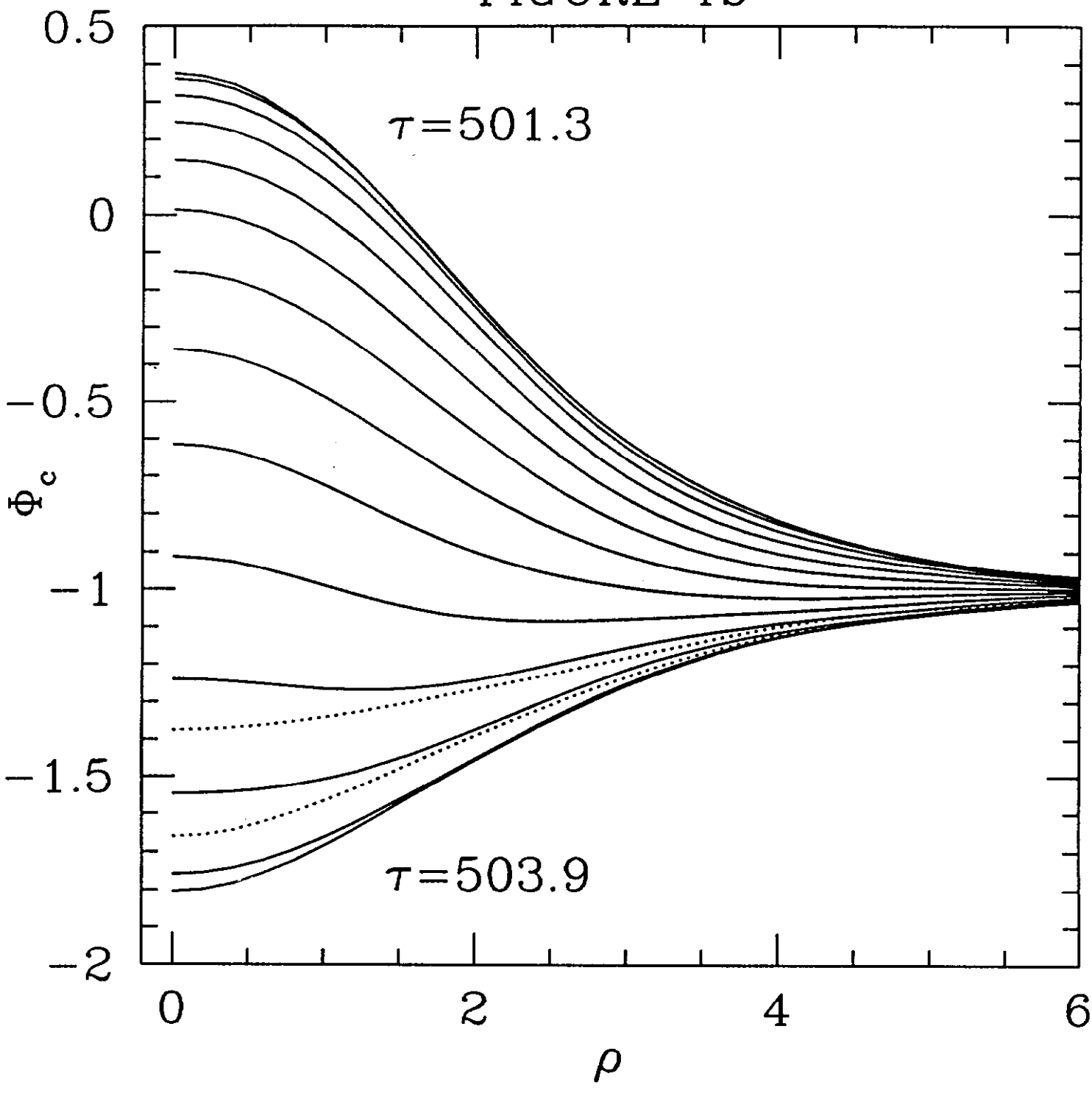

FIGURE 5

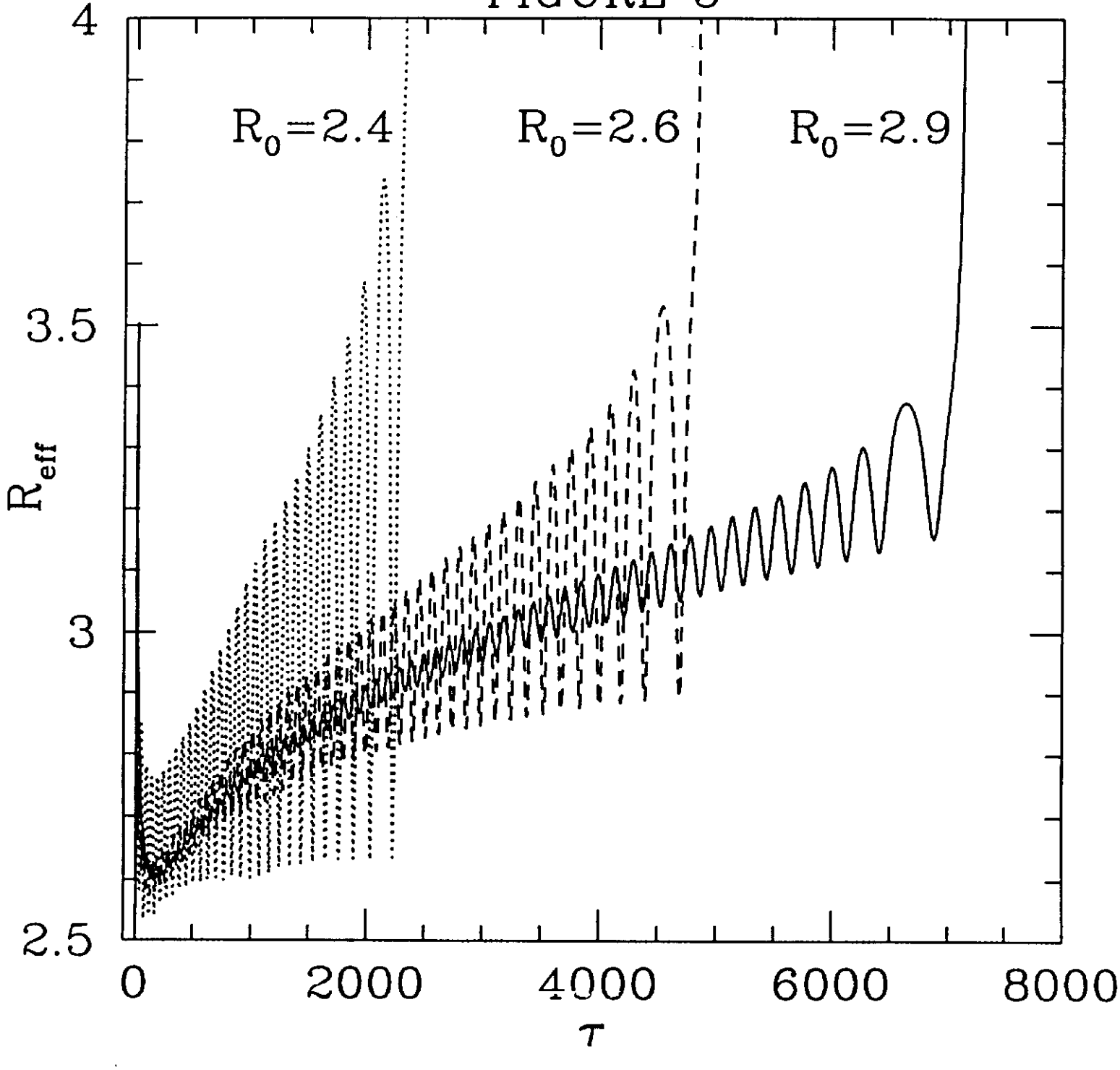

FIGURE 6a

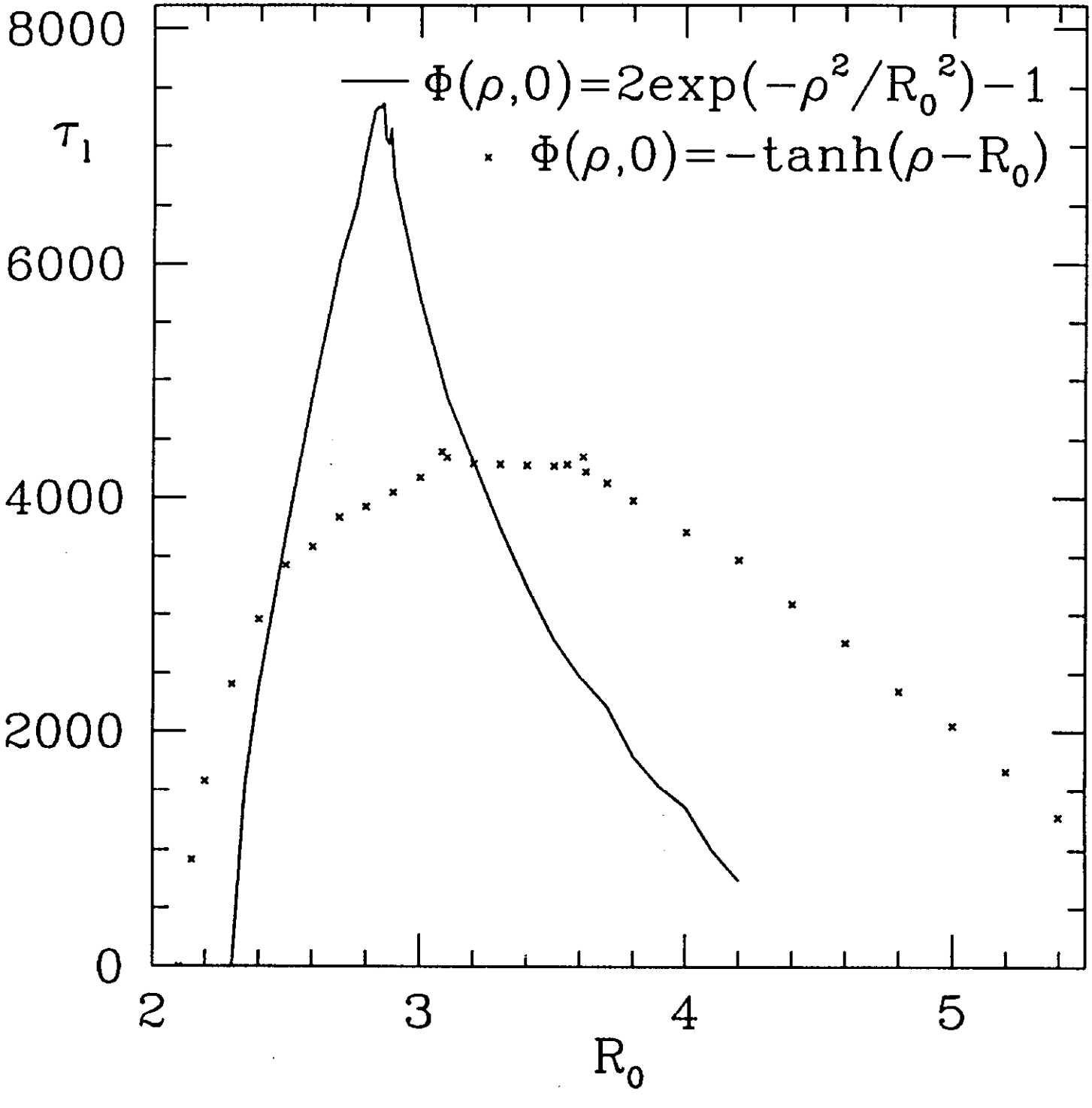
8000
6000
4000
2000
0
τ_1
$\Phi(\rho,0)=2\exp(-\rho^2/R_0^2)-1$
$\Phi(\rho,0)=-\tanh(\rho-R_0)$
2
3
4
5
R_0

FIGURE 6b

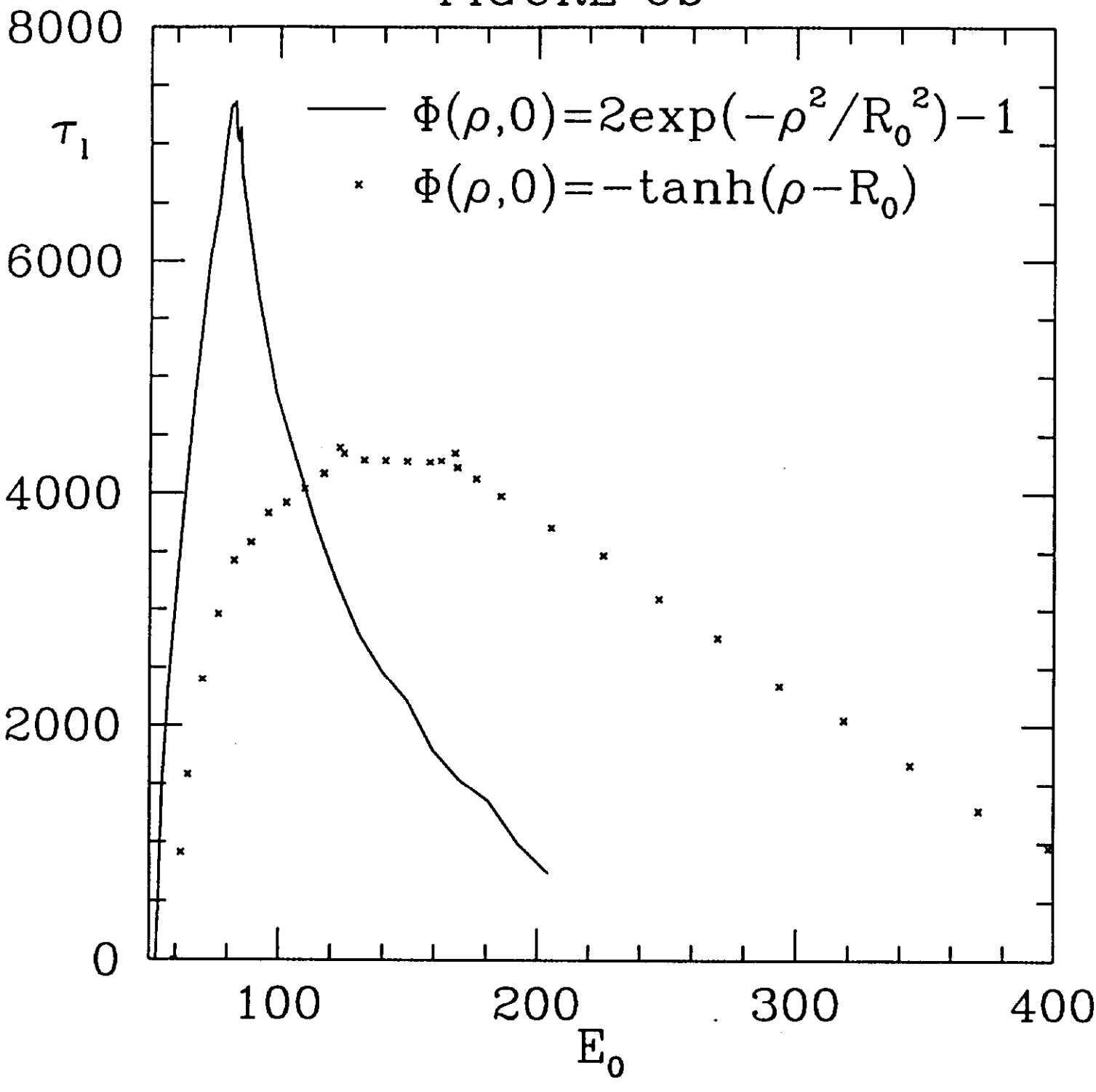
8000
6000
4000
2000
0
τ_1
$\Phi(\rho,0)=2\exp(-\rho^2/R_0^2)-1$
$\Phi(\rho,0)=-\tanh(\rho-R_0)$
100
200
300
400
E_0

FIGURE 7

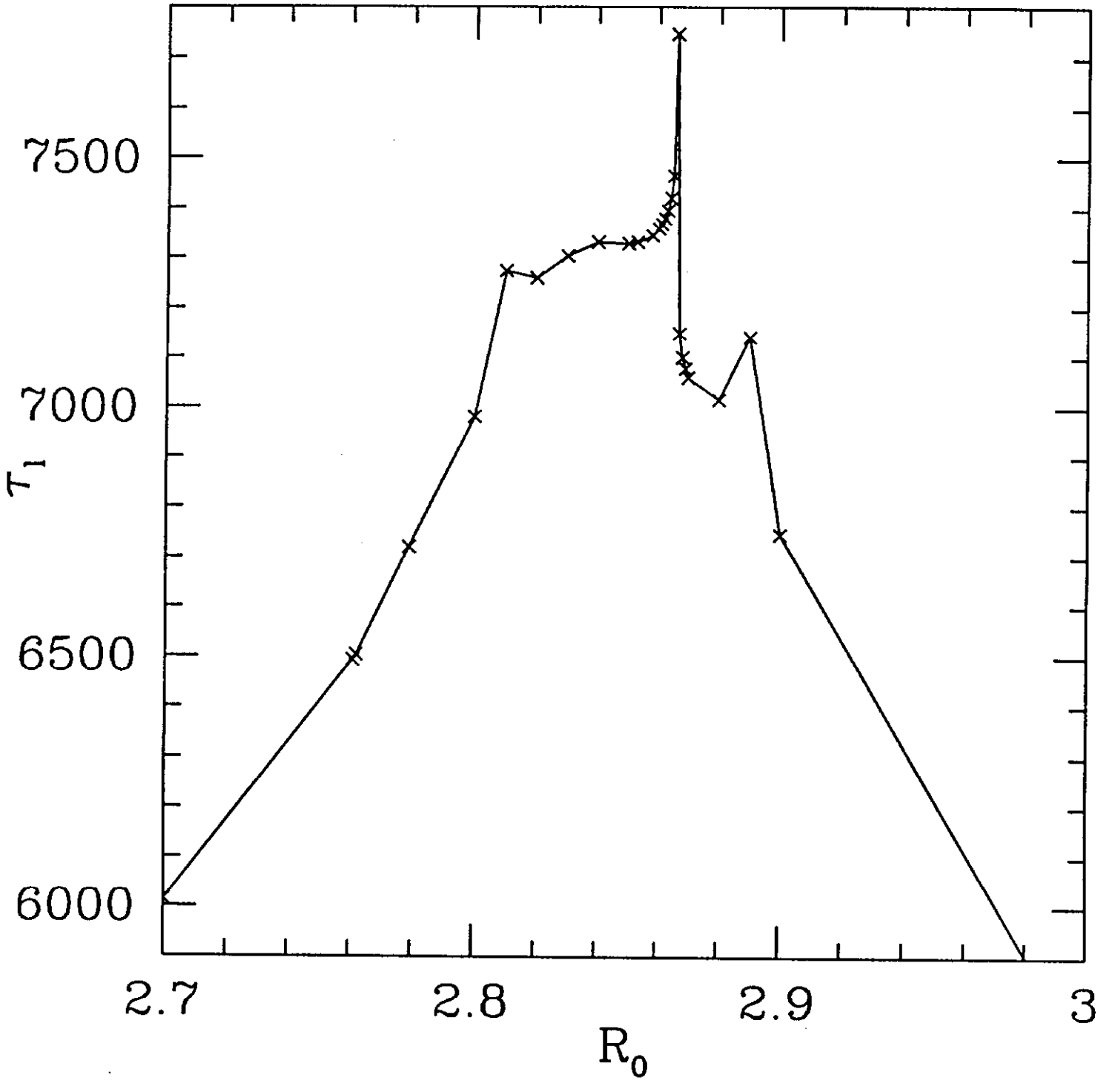

FIGURE 8a

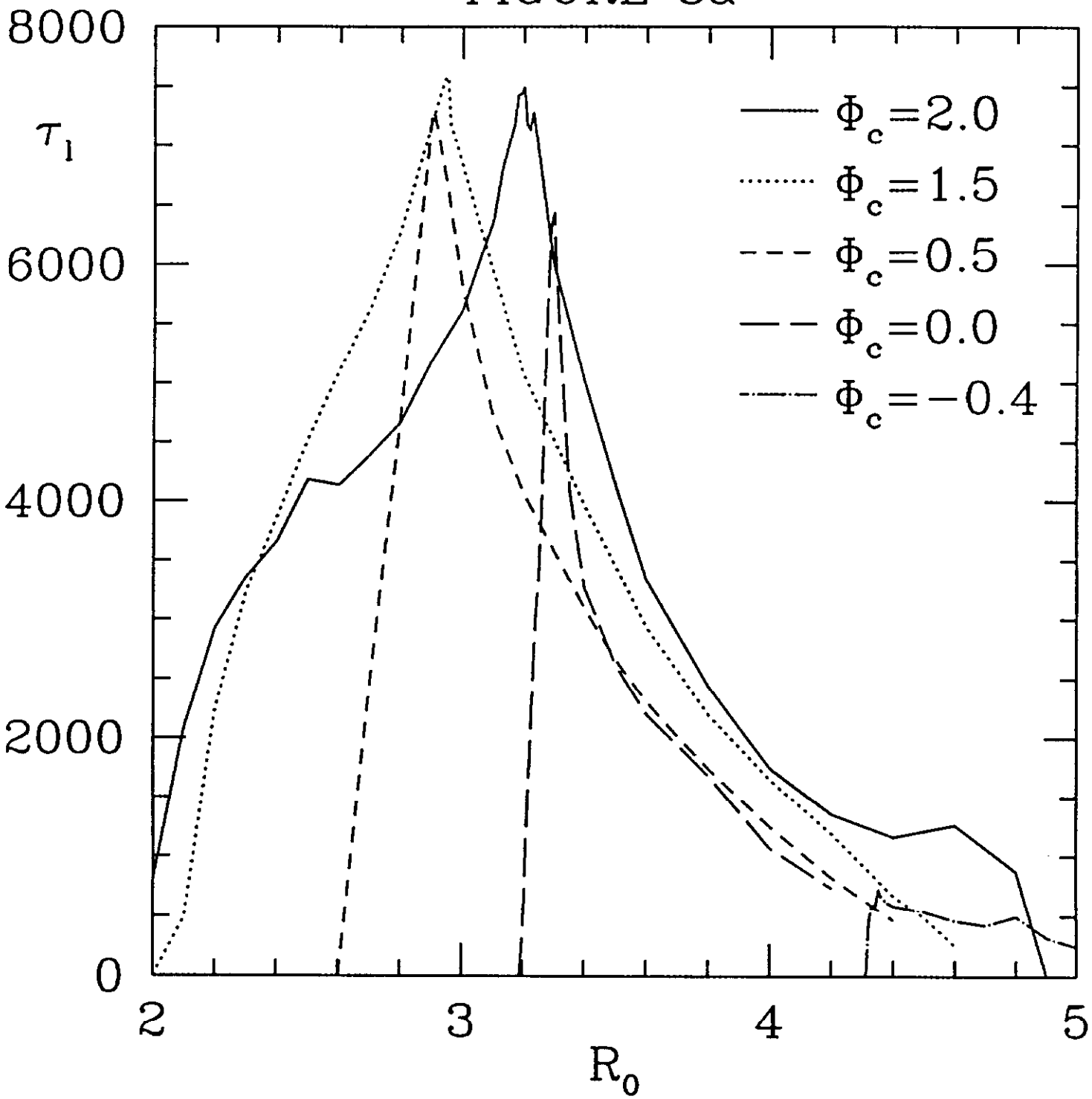
8000
6000
4000
2000
0
τ_1
2
3
4
5
R_0
Φ_c=2.0
Φ_c=1.5
Φ_c=0.5
Φ_c=0.0
Φ_c=−0.4

FIGURE 8b

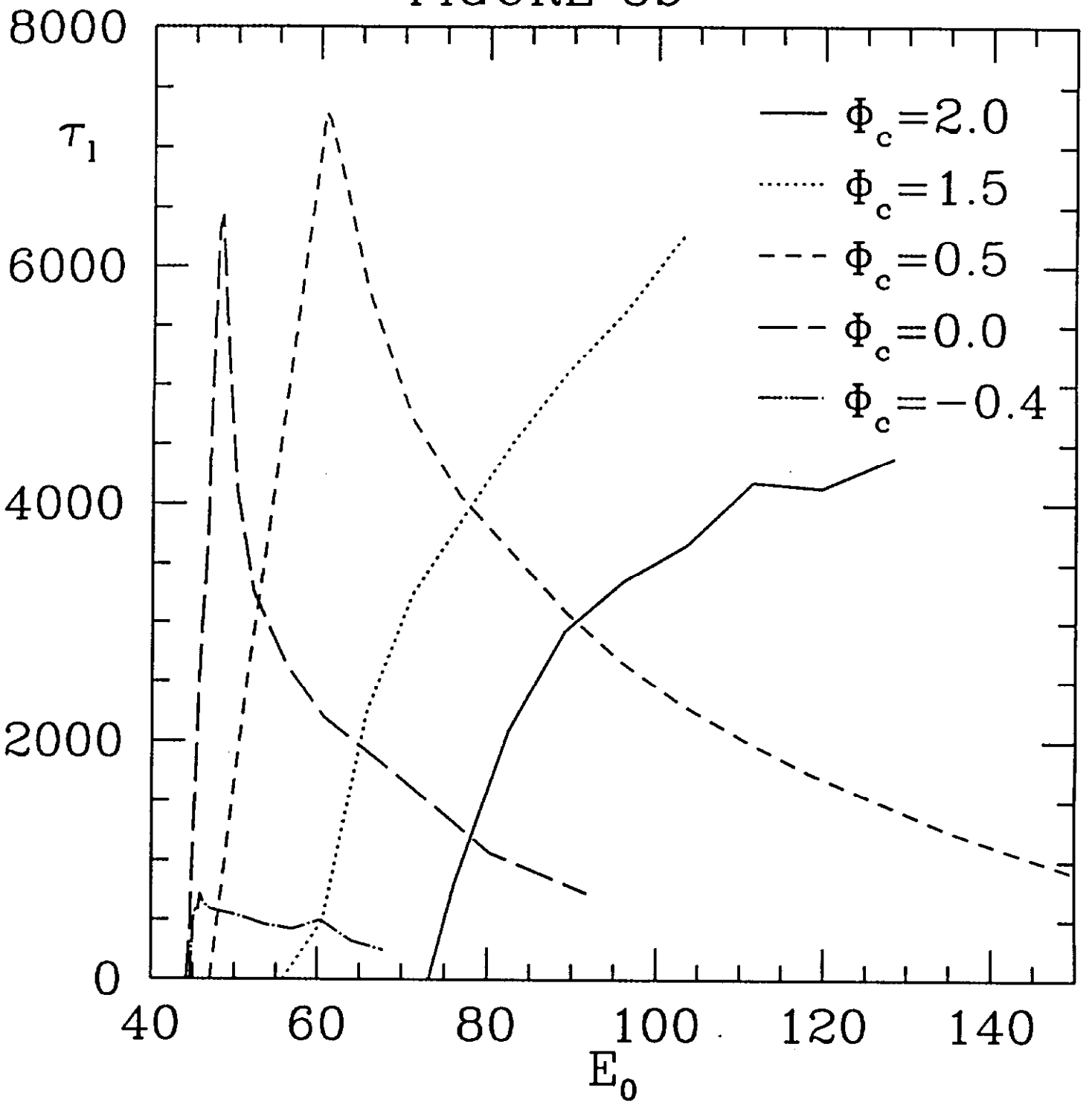
8000
6000
4000
2000
0
τ_1
40
60
80
100
120
140
E_0
Φ_c=2.0
Φ_c=1.5
Φ_c=0.5
Φ_c=0.0
Φ_c=−0.4

FIGURE 9

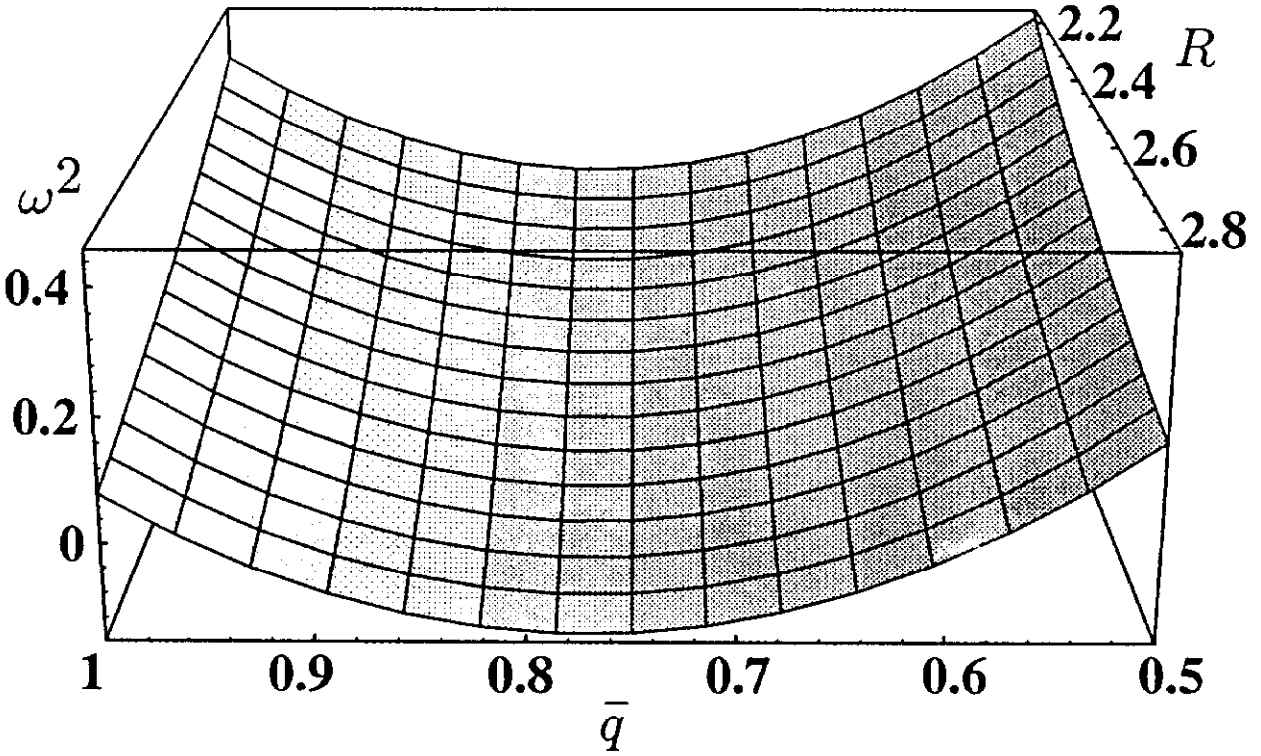

FIGURE 10

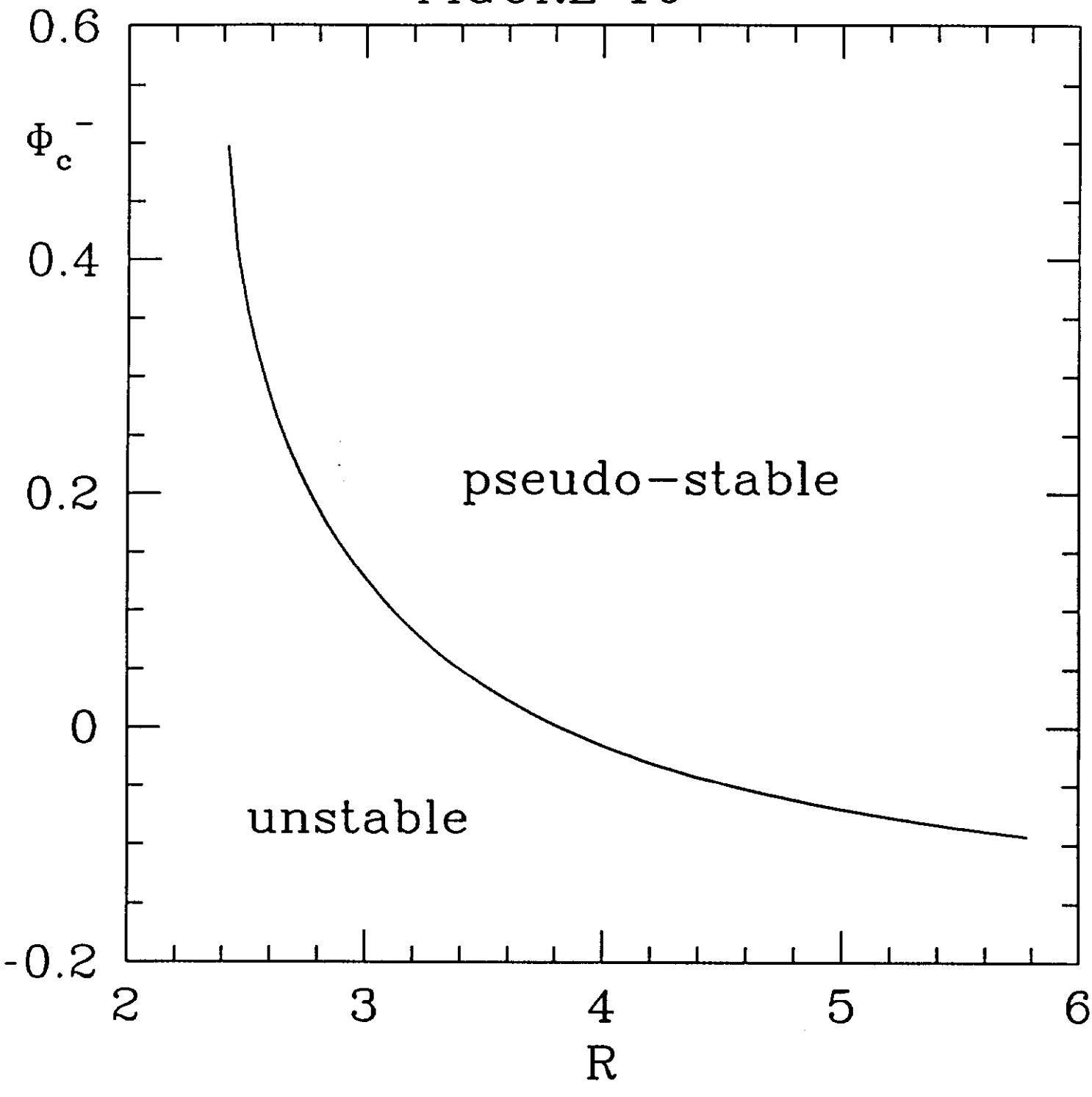

FIGURE 11

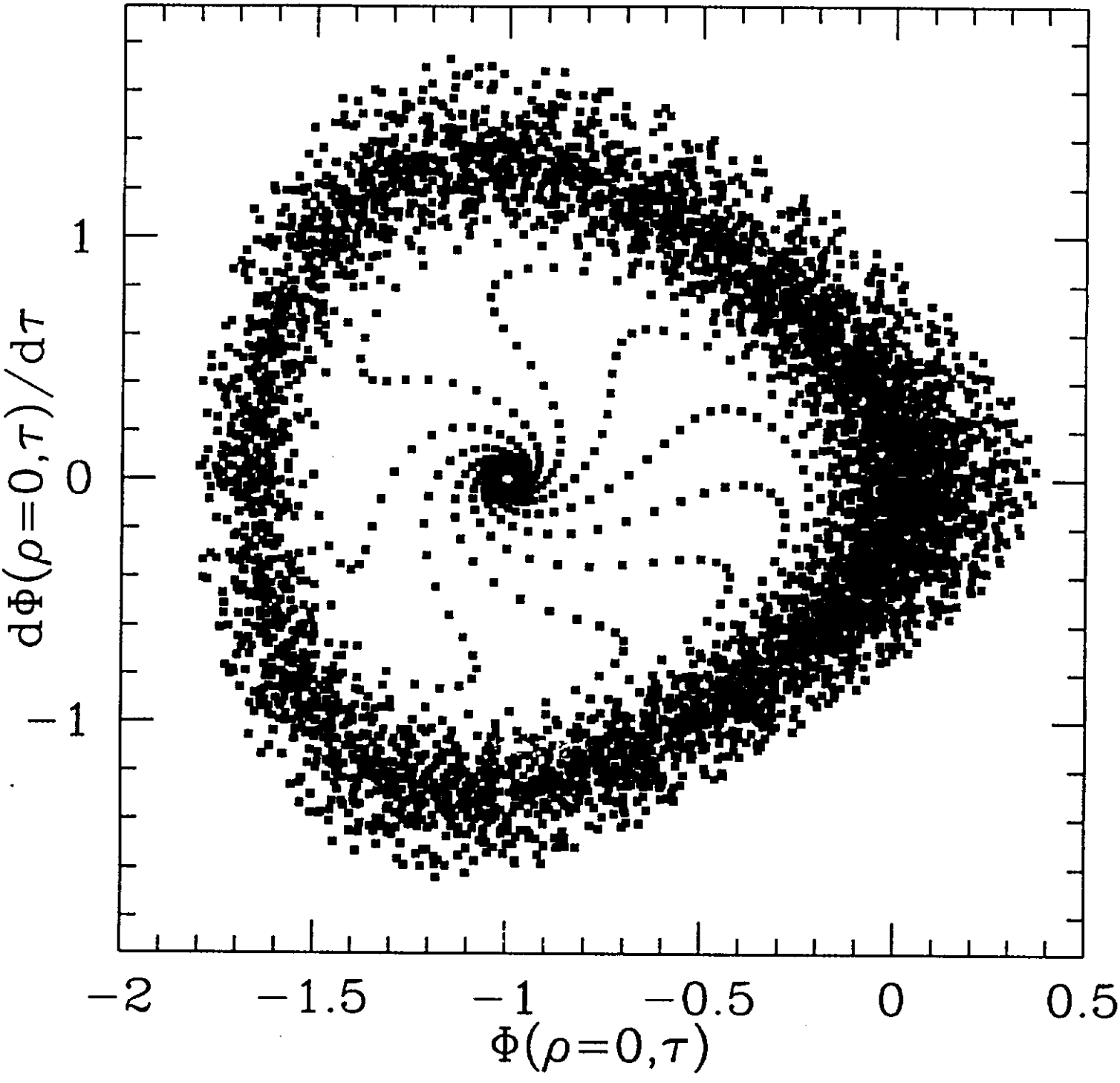

FIGURE 12

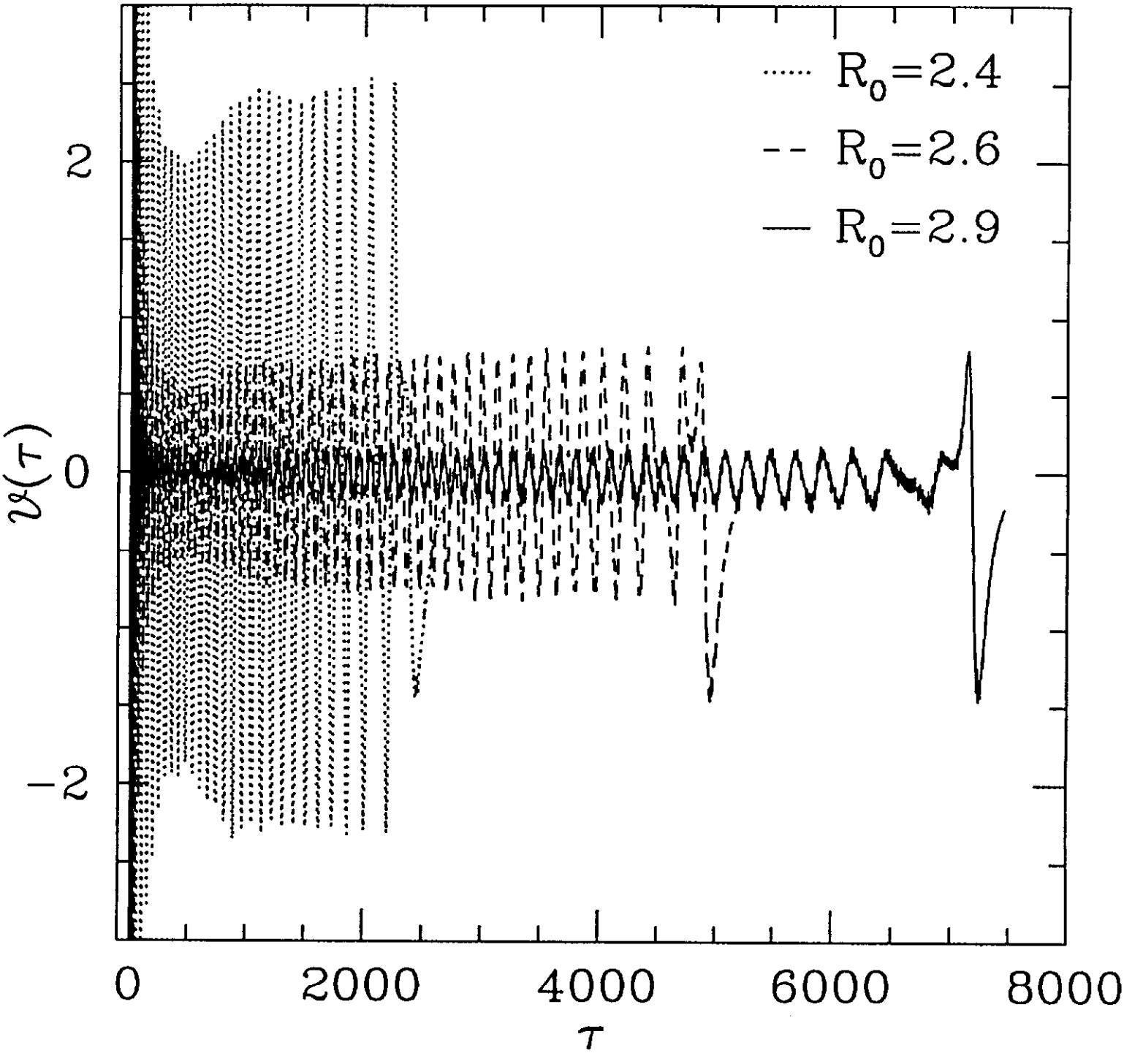

FIGURE 13

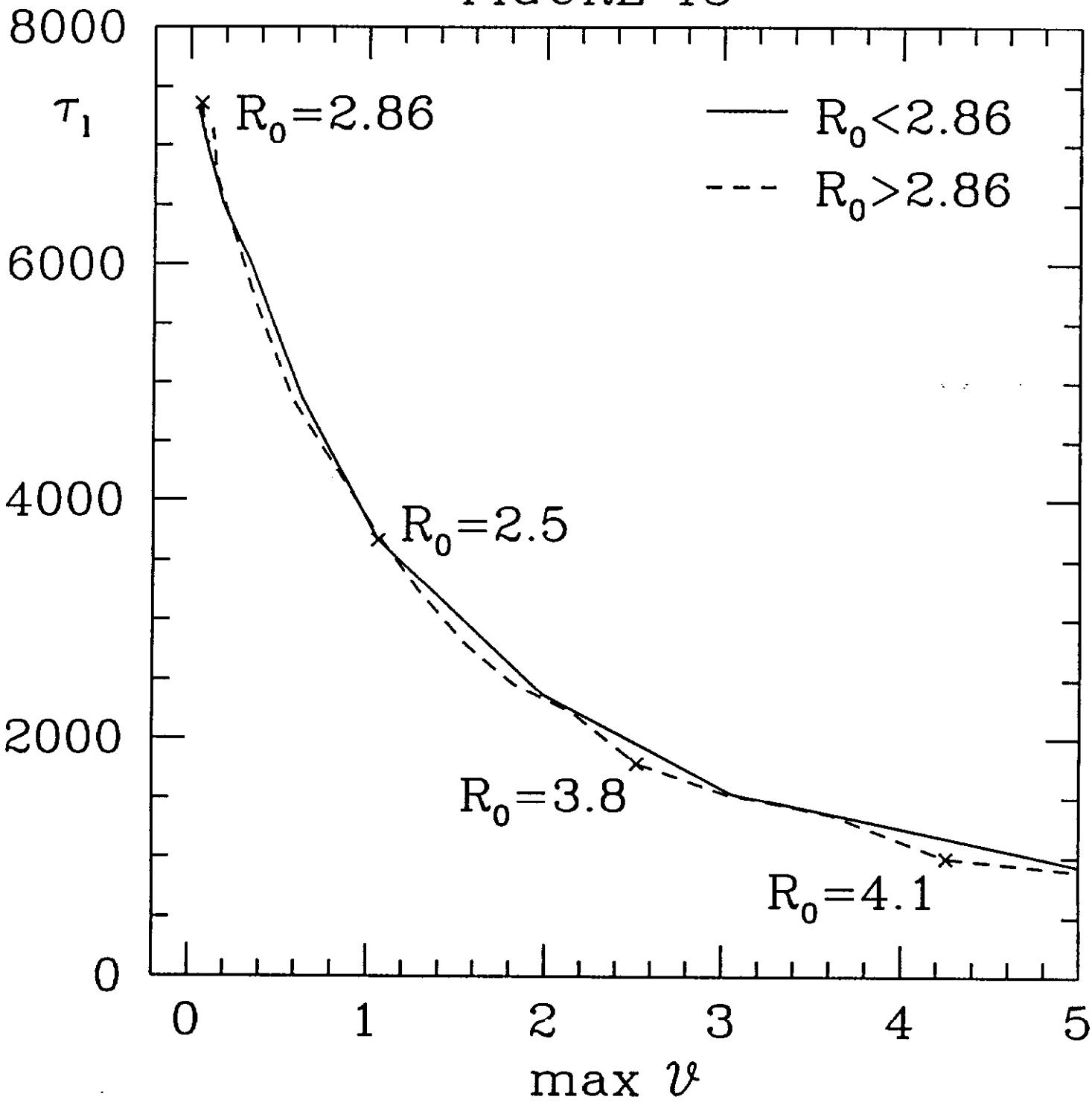
8000
6000
4000
2000
0
τ_1
R_0=2.86
R_0<2.86
R_0>2.86
R_0=2.5
R_0=3.8
R_0=4.1
0
1
2
3
4
5
max v

FIGURE 14

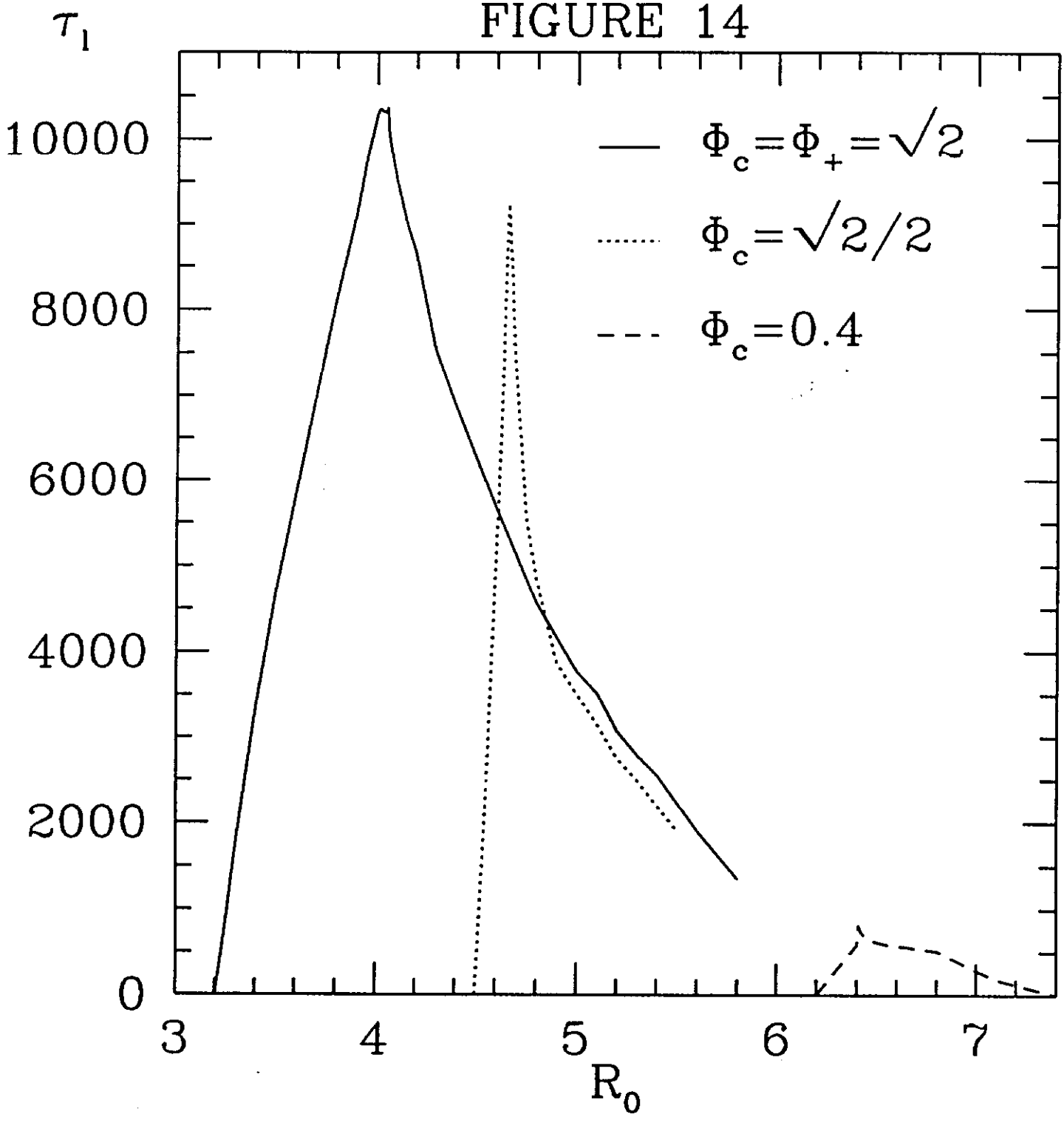
τ_1
10000
8000
6000
4000
2000
0
3
4
5
6
7
R_0
$\Phi_c=\Phi_+=\sqrt{2}$
$\Phi_c=\sqrt{2}/2$
$\Phi_c=0.4$

FIGURE 15a

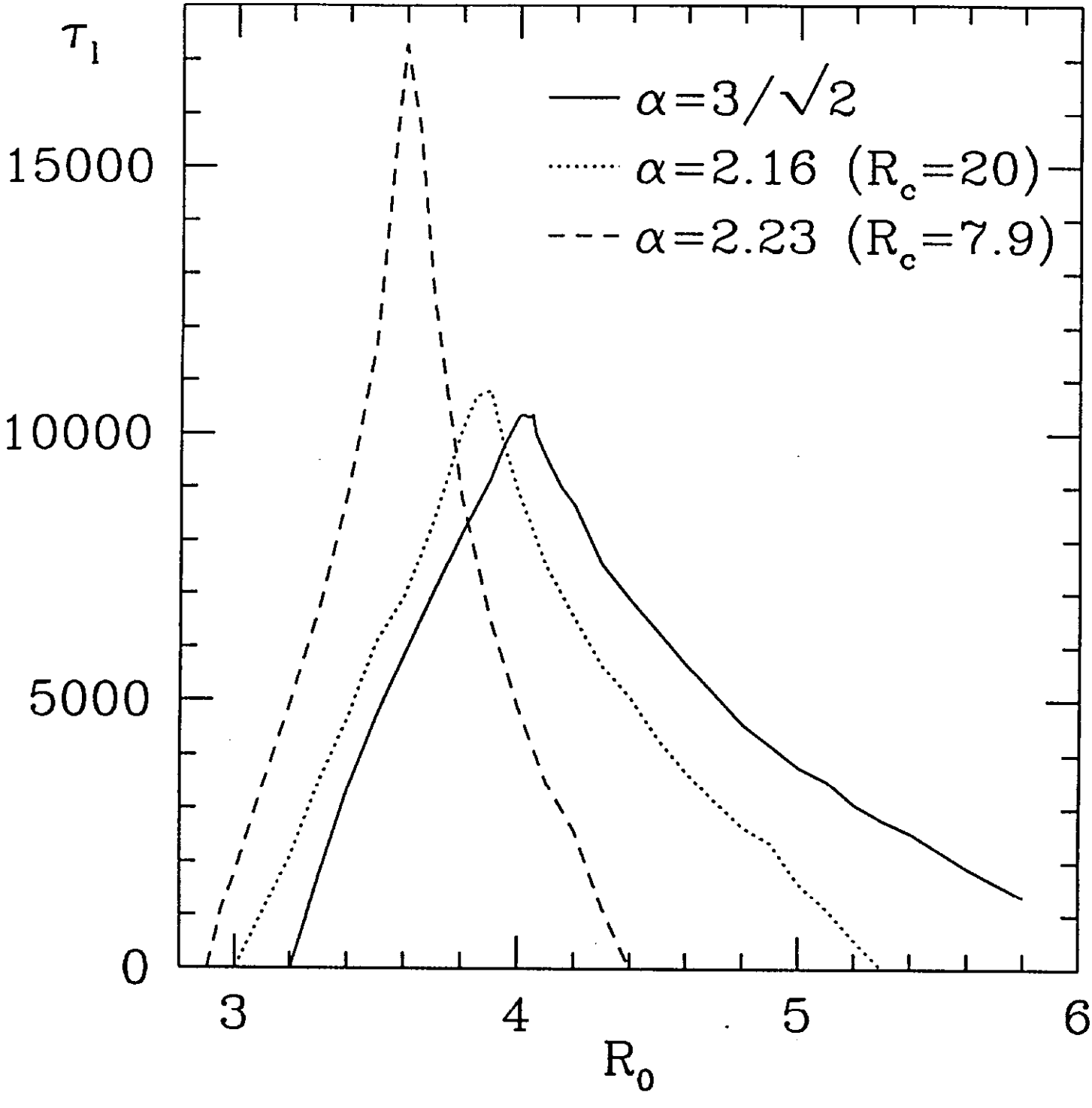
τ_1
15000
10000
5000
0
3
4
5
6
R_0
$\alpha=3/\sqrt{2}$
$\alpha=2.16$ ($R_c=20$)
$\alpha=2.23$ ($R_c=7.9$)

FIGURE 15b

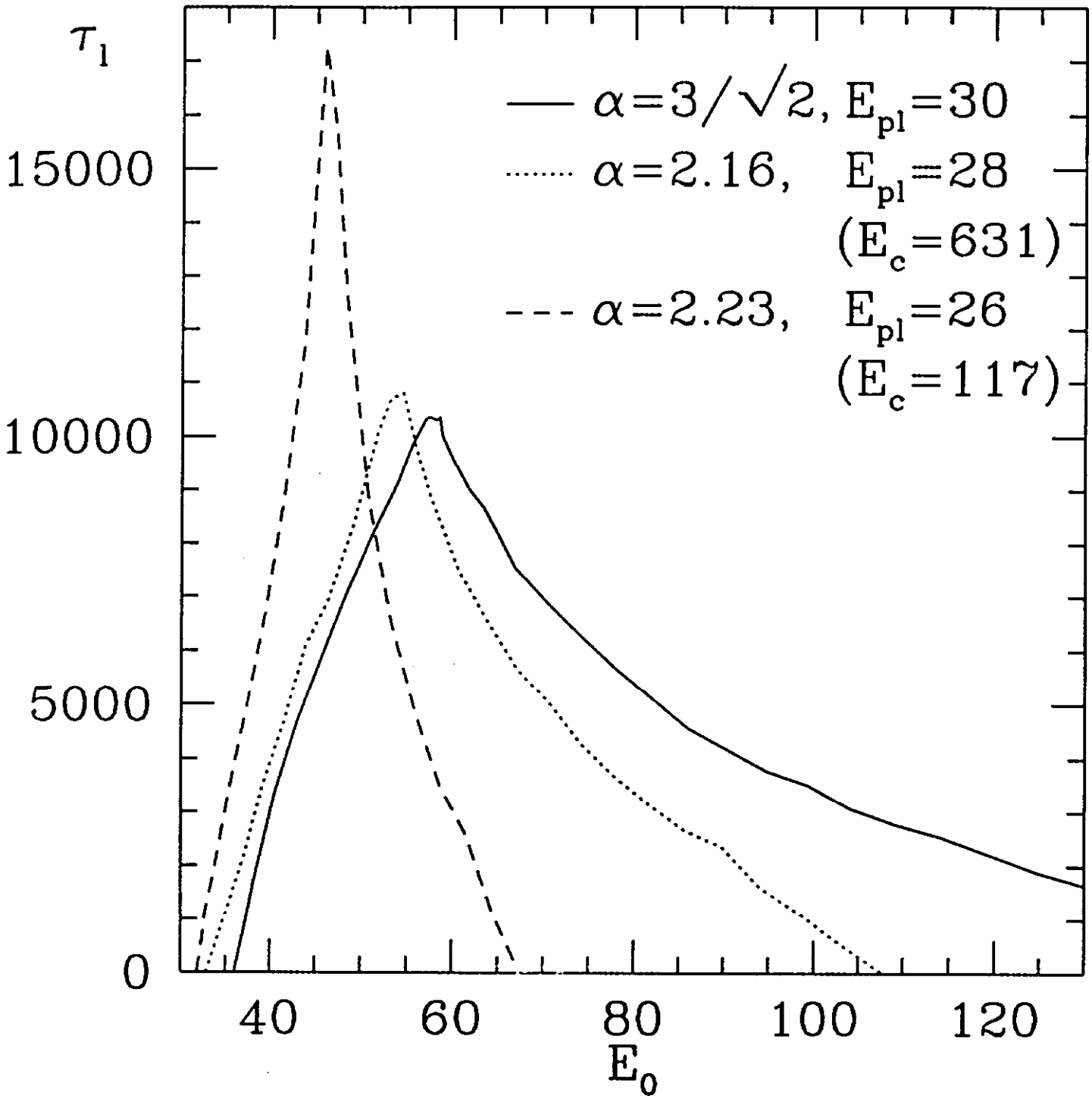
τ_1
15000
10000
5000
0
40
60
80
100
120
E_0
— $\alpha=3/\sqrt{2}$, $E_{pl}=30$
····· $\alpha=2.16$, $E_{pl}=28$
($E_c=631$)
--- $\alpha=2.23$, $E_{pl}=26$
($E_c=117$)